[redacted] CONFIDENTIAL

Copy
RM L57H16

NACA RM L57H16

CLASSIFICATION CHANGED
TO UNCLASSIFIED
By Authority of TD 7136 Date 12-15-70

NACA

RESEARCH MEMORANDUM

EXPERIMENTAL INVESTIGATION OF EFFECTS OF SIMULATED NACELLES AND WING-ROOT FREEDOMS ON SUPERSONIC FLUTTER CHARACTERISTICS OF A CAMBERED, MODIFIED, SWEPT, TAPERED WING

By Perry W. Hanson

Langley Aeronautical Laboratory
Langley Field, Va.

N71-70514
(ACCESSION NUMBER) (THRU)
44 None
(PAGES) (CODE)
(NASA CR OR TMX OR AD NUMBER) (CATEGORY)
FACILITY FORM 602

NATIONAL ADVISORY COMMITTEE
FOR AERONAUTICS

WASHINGTON
October 16, 1957

[redacted] CONFIDENTIAL

NATIONAL ADVISORY COMMITTEE FOR AERONAUTICS

RESEARCH MEMORANDUM

EXPERIMENTAL INVESTIGATION OF EFFECTS OF SIMULATED NACELLES AND WING-ROOT FREEDOMS ON SUPERSONIC FLUTTER CHARACTERISTICS OF A CAMBERED, MODIFIED, SWEPT, TAPERED WING

By Perry W. Hanson

SUMMARY

An experimental investigation has been made in the Langley 9- by 18-inch supersonic flutter tunnel to determine the effects of simulated engine nacelles and wing-root freedoms on the flutter characteristics of a cambered, modified, swept, tapered, semispan wing in the Mach number range from 1.3 to 3.0. Wing models were tested both with and without two nacelles with the model mount restrained, free to roll, and free to translate in the vertical direction. Normally, the simulated nacelles were attached immediately adjacent to the lower surface of the wing at 0.57- and 0.78-semispan stations, based on the exposed semispan, with the inboard-nacelle center of gravity at the 0.25-chord station and the outboard-nacelle center of gravity at the leading edge. Part of the investigation included determining the effects of moving the outboard-nacelle center of gravity back to the 0.25-chord station and to the 0.50-chord station.

The results indicate that the addition of nacelles at certain locations on the wing had a favorable effect on the flutter characteristics, whereas at other locations the effect was less favorable. The introduction of roll freedom and translation freedom in the wing mount proved beneficial under all conditions tested.

INTRODUCTION

The increased use of concentrated weights, such as engine nacelles, on highly swept wings has led to considerable interest in a study of

their effects on the wing flutter characteristics in the transonic and low-supersonic speed ranges. At the present time, analytical predictions of the flutter behavior of wings with concentrated weights and wing-root freedoms is uncertain. Therefore, the designer, to a large extent, must rely on experimentally determined flutter characteristics of a particular configuration that he may wish to use.

Accordingly, a limited investigation of the effects of concentrated weights and wing-root freedoms in the Mach number range from 1.3 to 3.0 has been made in the Langley 9- by 18-inch supersonic flutter tunnel by using semispan models of a proposed bomber-airplane wing. The purpose of this paper is to present the results of the investigation and to present the structural information describing the models.

Results are presented in reference 1 of a similar investigation in the transonic speed range which was made in the Langley transonic blowdown tunnel by using a full-span version of similar models.

SYMBOLS

a	speed of sound, ft/sec
b	wing semichord at 0.7-semispan station, based on exposed semispan, measured parallel to airstream, ft
c.g.	center of gravity
f_F	flutter frequency, cps
f_n	natural vibration frequency of nth mode, cps
I	mass moment of inertia, slug-ft^2
l	length of semispan of model, measured from and normal to root chord (chord at tunnel wall line), ft
m	mass, slugs
M	free-stream Mach number
q	free-stream dynamic pressure, lb/sq ft
T	free-stream temperature, $^\circ$R

y spanwise station, measured perpendicular to root chord from the root, ft

μ mass-ratio parameter (ratio of mass of exposed model to mass of volume of air contained in the solid generated by revolving each semichord about its midpoint, the length of the solid being the wing semispan)

ρ density of air in test section of tunnel, slugs/cu ft

ω_n frequency of vibration of nth mode, radians/sec

ω_α torsional frequency of vibration, radians/sec

APPARATUS AND TEST PROCEDURE

This investigation was made in the Langley 9- by 18-inch supersonic flutter tunnel which is a conventional, fixed-nozzle, blowdown wind tunnel exhausting into a vacuum sphere from a pressure reservoir. The nozzle configurations used gave Mach numbers of 1.3, 1.64, 2.0, and 3.0. At each Mach number the test-section density varies continuously to a controlled maximum density, and then decreases. The maximum test-section dynamic pressure obtainable varies from approximately 3,500 lb/sq ft at $M = 1.3$ to 3,900 lb/sq ft at $M = 1.64$ and 2.0; at $M = 3.0$, the maximum test-section dynamic pressure is 2,500 lb/sq ft.

For a given Mach number, the test procedure for all runs was essentially the same. The sphere to which the tunnel exhausts, and the test section, were pumped down to a pressure of approximately 2 lb/sq in. abs. The control valve upstream of the test section was then opened and the test-section density was allowed to increase until flutter was observed or the maximum density obtainable was reached.

The model-mount system was attached to the head of a ram that was used to inject and retract the models through one side of the test section. The wing was viewed through a window in the opposite side of the test section. Figure 1 is a photograph of one of the models mounted in the tunnel. The models were left-hand semispan wings which necessitated mounting them upside down since the flow is from the viewer's right.

Since the wing models had a cambered airfoil section, it was necessary to fly them at an angle of attack of approximately $1\frac{1}{2}^\circ$ to prevent failure due to lift loads when the model mount was restrained. With the model mount free to roll or free to translate vertically, the model was set at the angle of attack (determined by low-density trim runs) required

to center the wing-root clamp between the upper and lower stops on the mount. Two preliminary models not discussed in this report were expended in determining the optimum method of testing the cambered-airfoil models with mount freedoms.

The actual time for each run was approximately 4 to 5 seconds. A multichannel oscillograph provided a continuous record of the test conditions and of the behavior of a resistance wire strain-gage bridge attached to the wing surface. A high-speed (approximately 1,000 frames per second) 16-millimeter motion-picture camera furnished a record of the model motions.

MODELS

Nine semispan wings were used in the present investigation. All were of the same plan form and airfoil shape, but models 1 to 5 differed slightly from models 6 to 9 in construction details, the latter group being weaker and lighter than the former in order to obtain flutter data at the higher Mach numbers where the maximum tunnel density obtainable was not sufficient to produce flutter in models 1 to 5.

Geometry

The modified, swept, tapered wing had a 45° sweptback leading edge, an exposed panel aspect ratio of 1.67, and a taper ratio of 0.15 based on the wing-body intersection chord. The wing plan form incorporates a trailing-edge chord-extension over the inboard 35 percent of the semispan, as illustrated in figure 2. The basic airfoil section of the wing is a modified NACA 65-series cambered section whose coordinates are presented in table I. The coordinates for the midspan position are presented for the wing without the trailing-edge chord-extension. The true shape of the sections inboard of the 0.35-semispan station are obtained by fairing a tangent to the upper surface of the wing from the trailing edge of the extended chords. The plan form was formed by the addition of a straight-trailing-edge chord-extension to the inboard portion of a sweptback wing that had a panel aspect ratio of 1.81 and a taper ratio of 0.161. The modified NACA 65-series cambered airfoil sections of the swept wing (see table I) inboard of the 0.35-semispan station were further modified by fairing a tangent to the upper surface of the wing from the trailing edge of the extended chords. The streamwise thickness-chord ratios of the resulting airfoil sections varied from 0.04 at midspan to 0.03 at the tip. The wings were 0.022-size, dynamically and elastically scaled versions of a proposed airplane wing. The model mounts used established the wing-root boundary conditions but did not necessarily represent the mass and inertia properties of the fuselage.

The nacelles used consisted of conical forward and rearward sections with a cylindrical midsection and simulated the mass and inertia properties of the nacelles on the proposed wing. The nacelles (fig. 2) were rigidly attached immediately adjacent to the lower surface of the wing by means of two screws and were located at 0.57- and 0.78-semispan stations, based on the exposed semispan. Three nacelle configurations were tested. For one, considered the normal nacelle configuration, the inboard-nacelle center of gravity was at the 0.25-chord station and the outboard-nacelle center of gravity was at the leading edge. For the two special nacelle configurations, the outboard nacelle was moved back so that the center of gravity was at either the 0.25- or 0.50-chord station.

Construction

The main load-carrying structure for all the wings (figs. 2 and 3) consisted of a single formed-aluminum box spar, stabilized with foam plastic, to which perforated webs were attached. Wings 1 to 5 had aluminum ribs, magnolia-wood leading and trailing edges, and a box-spar wall thickness of 0.01 inch. Wings 6 to 9 did not have any aluminum ribs, had leading and trailing edges of balsa wood, and a box-spar wall thickness of 0.005 inch. Low-strength balsa was bonded to the framework to obtain the desired contour for all nine wings. Wings 1 to 5 were covered with Japanese tissue and aircraft dope, whereas wings 6 to 9 were covered with Mylar. One of the latter models is shown in figure 4. The simulated nacelles were turned from magnesium rods and were ballasted by lead weights as indicated in figure 2.

Mounts

Two separate mount assemblies were used in the present investigation. One mount allowed the wing to roll about the midspan chord and the other mount allowed the wing to translate vertically. Provision was made on each mount assembly to lock out the mount freedom. The roll mount assembly is shown in figure 5(a) and the translation mount assembly is shown in figure 5(b). The base blocks of both mount assemblies were bolted to a ledge on a ram which permitted injecting and retracting the model through the tunnel side wall. The wing was secured to each of the mount assemblies by the model mount, which held the root of the box spar and its flanges. For the roll mount assembly (see fig. 5(a)), the model mount was supported by two precision bearings which allowed movement in the roll direction only. A rearward extension of the model mount passed between two stop screws that were used either to limit the amount of roll or to lock out the roll movement entirely. The mount was held centered between the stop screws by two soft coil springs attached to the mount extension and secured to the mount-assembly frame above and below the beam. Contact with either of the stop screws was indicated through a

set of fouling switches which operated a fouling light outside the tunnel and displaced a trace on the oscillograph record of the run. The model mount on the translation mount assembly (see fig. 5(b)) was attached to a parallelogram linkage by means of eight small precision ball bearings. This parallelogram linkage permitted freedom in vertical translation only. As in the roll mount assembly, stop screws above and below the model mount limited or restrained the vertical motion; and contact of the model mount with either of the stop screws was indicated by fouling switches not visible in the photograph. The model was centered in the mount by two springs attached to the model mount from above and below. The model-mount cover plate was common to both mount assemblies; it provided 1/4-inch clearance around the wing at the root chord when the wing was centered in the mount and, with the model fully injected in the tunnel, was flush with the tunnel wall.

Physical Properties

The bare-wing masses and the natural frequencies of the wings under the various test conditions are presented in table II. The mass and inertia properties of the basic nacelles used with the various wings are presented in table III. The mass and inertia properties of a wing representative of models 1 to 5 are presented in table IV, and the segmented mass distribution is presented in table V. These data are from reference 1 and are presented here for completeness. The mass distribution of a wing representative of models 6 to 9 is presented in table VI. In working up the mass data for wings 6 to 9 it was decided that it was desirable to obtain more information on the chordwise mass distribution. Hence, the wing was divided into four chordwise sections and eight spanwise stations. Only mass data are presented since the moments of inertia of the segments may be neglected in a flutter analysis if the segments are small enough. Attachment screws not included in the basic nacelle data shifted the center of gravity rearward 0.03 to 0.04 inch. Typical node lines for the wings under all the test configurations used are shown in figure 6. Representative mode shapes, obtained by the method of reference 2, for the two series of wings with and without the normal nacelle configuration and with the mount restrained are shown in figures 7 to 10 as three-dimensional drawings of the deflected models. A table of normalized deflections at the various locations is presented with each mode shape. The chordwise divisions inboard of the 0.35-semispan station are based on hypothetical chord lengths determined by extending to the root the trailing edge outboard of the 0.35-semispan station. The wing tip is on the viewer's right when looking from the trailing edge toward the leading edge.

RESULTS AND DISCUSSION

General

The results of the tests are presented in table VII except for model 9 which was destroyed by lifting loads early in the run because of an incorrect angle-of-attack setting. The natural frequency of vibration ω_α used in the altitude-stiffness parameter $\frac{b\omega_\alpha}{a}\sqrt{\mu}$ is taken as the frequency of the mode most nearly resembling the first torsion mode. For the wings with nacelles, $\omega_\alpha = \omega_2$; and for the wing without nacelles, $\omega_\alpha = \omega_3$.

Effect of Nacelles

The dynamic pressure at flutter or the maximum dynamic pressure obtained in tests where the wing could not be fluttered is plotted against Mach number in figure 11. The small numbers beside each symbol identify data points in table VII. From this figure it can be seen that at $M = 1.3$ and with the wing mount restrained, the addition of nacelles in the normal configuration raised the dynamic pressure necessary for flutter from 1,520 lb/sq ft to 2,770 lb/sq ft, an increase of approximately 82 percent. With the mount restrained, at $M = 1.64$, the addition of nacelles in the normal configuration raised the critical dynamic pressure from 2,263 lb/sq ft to a value above 3,900 lb/sq ft, the maximum dynamic pressure obtained at $M = 1.64$. This is an increase of at least 72 percent. At $M = 2.0$ with the mount restrained, adding nacelles in the normal configuration raised the critical dynamic pressure from 2,530 to 3,488 lb/sq ft, an increase of approximately 38 percent. As a matter of interest, the results of reference 1 indicated that at $M = 0.65$ the addition of nacelles to the wing with the mount restrained increased the critical dynamic pressure by 70 percent. No flutter was obtained at $M = 3.0$ with the mount restrained either with the bare wing or with the normal nacelle configuration up to the maximum dynamic pressure of approximately 2,400 lb/sq ft.

A limited investigation was undertaken to determine the effect of shifting the nacelle centers of gravity in the chordwise direction. Because of the limited number of models available, this portion of the investigation was confined to moving the outboard nacelle (and, therefore, the center of gravity) rearward to the 0.25-chord station at $M = 1.3$ with the mount both restrained and free to roll, and to the 0.50-chord station at $M = 1.3$ and $M = 1.64$ with the mount restrained only. From figure 11 it can be seen that at $M = 1.3$ moving the outboard nacelle center of gravity from the normal location at the leading

edge back to the 0.25-chord station lowered the critical dynamic pressure from 2,770 to 2,200 lb/sq ft, a difference of 21 percent. Moving the nacelle center of gravity rearward to the 0.50-chord station at the same Mach number further reduced the critical dynamic pressure to 1,800 lb/sq ft, 35 percent less than the critical dynamic pressure for the normal nacelle configuration. At $M = 1.64$, moving the outboard nacelle center of gravity rearward to the 0.50-chord station reduced the critical dynamic pressure from a value above 3,800 lb/sq ft for the normal nacelle configuration to 2,890 lb/sq ft, a reduction of only 24 percent compared with the 35-percent reduction at $M = 1.3$.

Flutter Boundary

If the altitude-stiffness parameter $\frac{b\omega_\alpha}{a}\sqrt{\mu}$ at flutter is plotted against Mach number for the bare-wing condition with the mount restrained, a flutter boundary is established. This is shown as the upper curve in figure 12. Further, it is interesting to note that, when μ is determined for the wings with nacelles by using the mass of the wing and nacelles together, the shape of the flutter-boundary curve is essentially the same as that of the bare wing but lower by approximately 70 percent. The region below the curves is the flutter region. It should be noted that, in testing a wing at a particular Mach number in the tunnel, the flight path approaches the flutter boundary vertically from top to bottom in figure 12.

Effect of Wing-Mount Freedom

An attempt was made to determine the effect of allowing the wing mount to have freedom to roll and freedom to translate vertically. From figure 11 it can be seen that the introduction of either roll or translation freedom to the wing mount at $M = 1.3$ raised the flutter dynamic pressure to a value above the maximum pressure obtainable in the tunnel for both the bare wing and wing with the normal nacelle configuration. Introducing roll freedom in the mount for the wing with the outboard nacelle center of gravity at the 0.25-chord station had negligible effect on the flutter dynamic pressure: the pressure was raised from 2,200 lb/sq ft for the mount-restrained condition to 2,210 lb/sq ft for the mount-free-to-roll condition. At $M = 2.0$, no flutter was obtained for the wing with the normal nacelle configuration up to a dynamic pressure of 3,620 lb/sq ft with the wing mount free to roll and up to 3,500 lb/sq ft for the wing mount free to translate. These were the maximum dynamic pressures obtainable. No flutter was obtained at $M = 3.0$ under any of the configurations tested.

CONCLUSIONS

The following conclusions are presented from an experimental investigation of the effects of simulated nacelles and wing-root freedoms on the supersonic flutter characteristics of a cambered, modified, swept, tapered wing at Mach numbers from 1.3 to 3.0:

1. At the Mach numbers M tested with the wing mount restrained, the addition of nacelles in the normal configuration raised the flutter dynamic pressure by at least 82 percent at $M = 1.3$, by at least 72 percent at $M = 1.64$, and by 38 percent at $M = 2.0$.

2. With the wing mount restrained, moving the outboard-nacelle center of gravity rearward to the 0.25-chord station at $M = 1.3$ reduced the flutter dynamic pressure for the normal nacelle configuration by 21 percent. Further movement of the outboard-nacelle center of gravity rearward to the 0.50-chord station reduced the flutter dynamic pressure by 35 percent at $M = 1.3$ and by at least 24 percent at $M = 1.64$.

3. Introduction of either roll or translation freedom to the wing mount for both the bare wing and the wing with the normal nacelle configuration raised the flutter dynamic pressure to values above the maximum pressure obtainable in the tunnel for the Mach numbers tested. Introduction of roll freedom to the mount for the wing with the outboard nacelle center of gravity at the 0.25-chord station had negligible effect on the flutter dynamic pressure at $M = 1.3$.

Langley Aeronautical Laboratory,
National Advisory Committee for Aeronautics,
Langley Field, Va., July 31, 1957.

REFERENCES

1. Kelly, H. Neale: Transonic Flutter Characteristics of a Cambered A-Plan-Form Wing With and Without Simulated Nacelles. NACA RM L57E09, 1957.

2. Hanson, Perry W., and Tuovila, W. J.: Experimentally Determined Natural Vibration Modes of Some Cantilever-Wing Flutter Models by Using an Acceleration Method. NACA TN 4010, 1957.

TABLE I

STREAMWISE AIRFOIL ORDINATES

[Dimensions are in inches]

Root (at midspan) (a)			Tip		
Abscissa	Ordinate		Abscissa	Ordinate	
	Upper	Lower		Upper	Lower
0	0.005	0	0	0	0
.189	.079	.026	.028	.008	.003
.377	.118	.030	.057	.012	.003
.755	.167	.039	.113	.017	.004
1.132	.197	.048	.170	.020	.005
1.509	.216	.056	.226	.022	.006
2.264	.238	.073	.340	.025	.008
3.019	.244	.084	.453	.025	.009
3.774	.234	.083	.566	.024	.009
4.528	.206	.070	.679	.021	.007
5.283	.163	.053	.792	.017	.005
6.038	.111	.035	.906	.012	.004
6.792	.056	.018	1.019	.006	.002
7.547	.003	.002	1.132	.003	.002
Leading-edge radius: 0.013			Leading-edge radius: 0.0014		

[a]Wing without trailing-edge chord-extension.

CONFIDENTIAL

TABLE II

BARE-WING MASSES AND WING NATURAL FREQUENCIES

UNDER VARIOUS TEST CONDITIONS

Model	Bare-wing mass, slugs	Bare-wing frequency, cps			Frequency of wing with normal nacelle configuration, cps				Frequency of wing with outboard nacelle at 0.25-chord station, cps				Frequency of wing with outboard nacelle at 0.50-chord station, cps				Mount condition
		f_1	f_2	f_3	f_1	f_2	f_3	f_4	f_1	f_2	f_3	f_4	f_1	f_2	f_3	f_4	(a)
1	0.002360	101	300	467	69	181	273										C
1	.002360	[b]205	[b]275	[b]466	165	[b]228	275	396									R
2	.002200	81	290	467	72	181	297	390									T
3	.002365	105	335	500	74	188	298	410					60	191	290	320	C
3	.002365				80	180	306										T
4	.002133				163	228	[b]272	398									R
5	.002155				69	184	280	322	63	197	285	396	60	184	285	303	C
5	.002155								142	225	270	390					R
6	.001990	85	265	450	58	139	236	325									C
7	.002130				60	147	240	320									C
8	.002070	89	280	456													C
9	.002097	88	277	470													C

[a]Code used in table is defined as follows:

C model mount restrained
R model mount free to roll
T model mount free to translate

[b]Frequencies determined with wing-mount assembly clamped to a back stop rather than in the tunnel (model mount free to roll).

CONFIDENTIAL

TABLE III

MASS AND INERTIA PROPERTIES OF NACELLES

WITHOUT ATTACHMENT SCREWS

Model	Outboard nacelle		Inboard nacelle	
	Mass, slugs	I_{cg}, slug-ft^2	Mass, slugs	I_{cg}, slug-ft^2
1	6.71×10^{-4}	4.75×10^{-6}	6.80×10^{-4}	4.53×10^{-6}
2	6.62	4.75	6.86	4.75
3	6.71	4.75	6.71	4.96
4	6.83	4.75	6.71	4.75
5	6.71	4.75	6.71	4.96
6	6.65	4.96	6.86	4.53
7	6.62	4.75	6.86	4.75

TABLE IV

MASS AND INERTIA PROPERTIES OF WING REPRESENTATIVE OF MODELS 1 TO 5

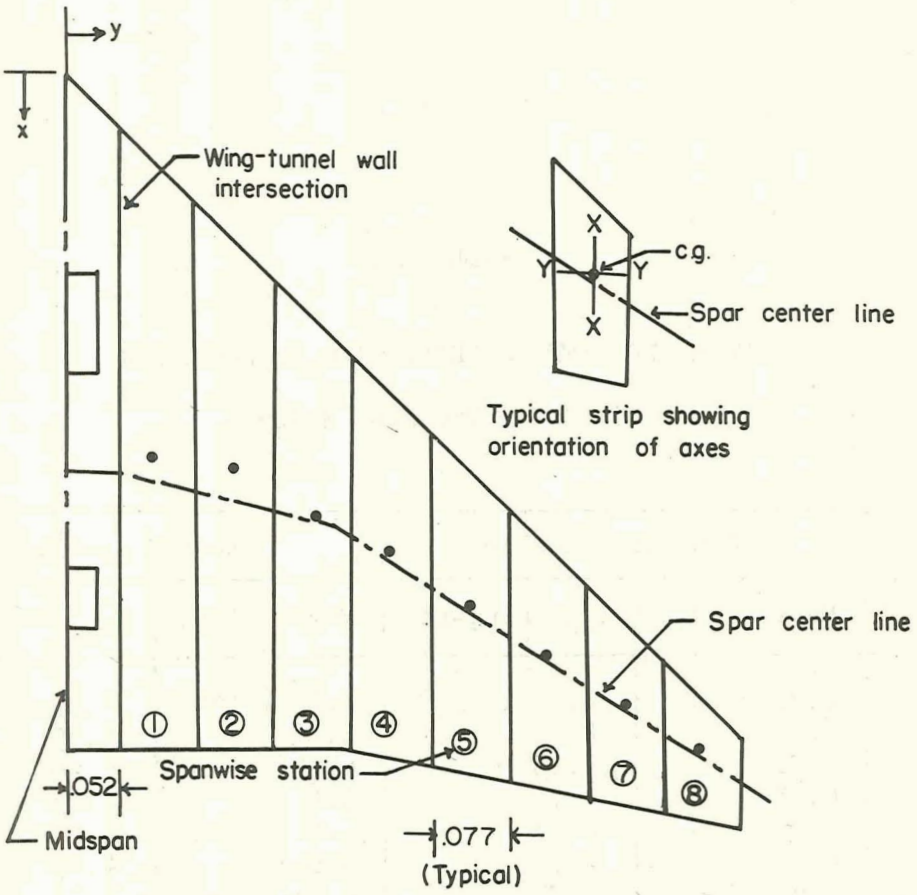

Spanwise station	Mass, slugs	c.g. location, in.		$I_{c.g.} \times 10^6$, slug-ft^2	
		x	y	Y - Y	X - X
1	0.000584	4.65	1.06	12.65	0.32
2	.000448	4.80	1.95	7.36	.24
3	.000357	5.36	2.92	3.69	.19
4	.000298	5.76	3.83	2.29	.15
5	.000255	6.42	4.77	1.19	.13
6	.000190	6.98	5.66	.65	.11
7	.000149	7.55	6.62	.26	.06
8	.000081	8.13	7.49	.08	.04

TABLE V

SEGMENTED MASS DISTRIBUTION OF WING REPRESENTATIVE OF MODELS 1 TO 5

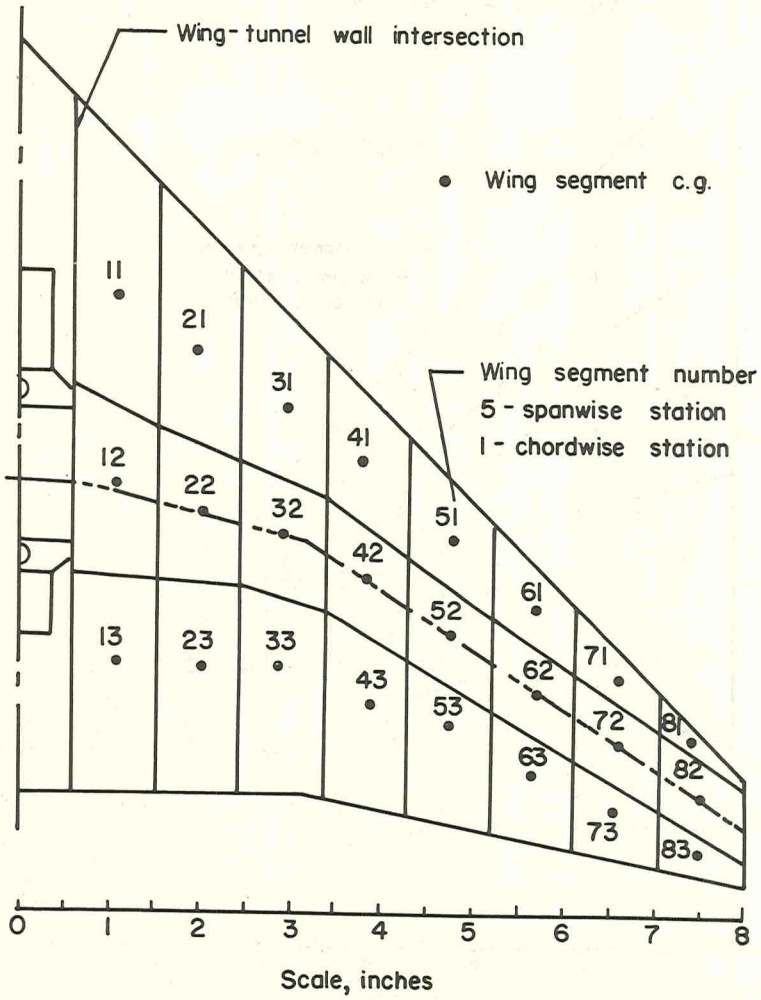

	Mass of wing segments (slugs x 10^6)							
Chordwise station	Spanwise station							
	1	2	3	4	5	6	7	8
1	209.9	189.7	115.6	99.9	64.3	48.1	31.4	10.0
2	207.1	154.6	142.8	131.1	136.7	105.0	101.8	64.9
3	172.2	112.3	106.0	73.7	59.6	39.0	19.5	6.4

TABLE VI

MASS AND INERTIA PROPERTIES OF WING REPRESENTATIVE OF MODELS 6 TO 9

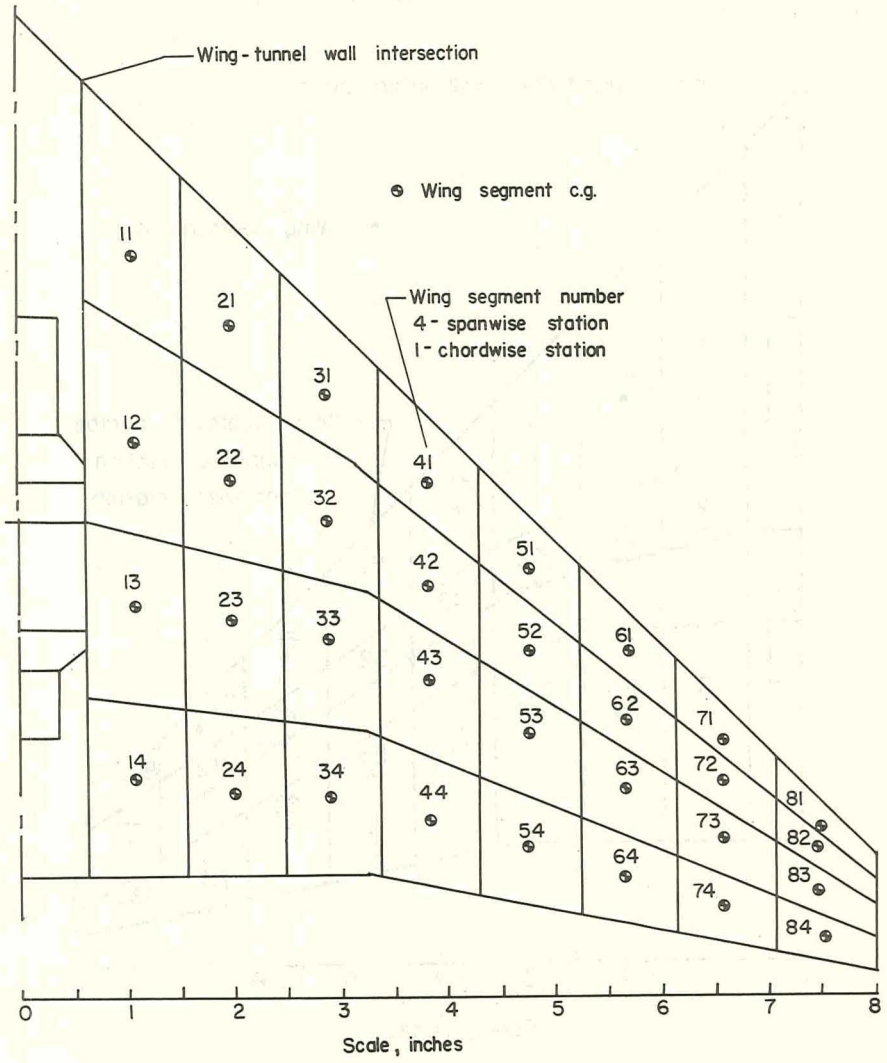

Chordwise station	Mass of wing segments (slugs x 10^6)							
	Spanwise station							
	1	2	3	4	5	6	7	8
1	82.8	65.0	42.4	38.3	34.9	24.6	21.2	20.5
2	202.0	152.0	119.7	101.3	85.6	63.0	46.5	23.9
3	156.0	117.0	108.2	89.7	76.7	63.0	50.0	32.2
4	53.4	39.0	28.7	24.0	19.2	17.1	11.6	11.0

TABLE VII

EXPERIMENTAL RESULTS

Data point	Model	Mount condition (a)	Nacelle configuration (a)	M	f_F, cps (a)	ρ, slugs/cu ft	T, °R	q, lb/sq ft	a, ft/sec	$\sqrt{\mu}$	$\frac{b\omega_\alpha}{a}\sqrt{\mu}$
1	3	T	N	3.00	Q	9.67×10^{-4}	601	2,080	691	7.41	1.47
2	3	C	N	3.00	Q	9.70	620	2,320	730	7.40	1.45
3	3	C	B	3.00	Q	10.00	617	2,400	726	5.81	3.04
4	4	R	N	3.00	Q	9.80	623	2,355	731	7.14	1.69
5	4	R	N	2.00	Q	24.00	566	3,620	869	4.56	.91
6	3	T	N	2.00	Q	22.80	578	3,500	877	4.83	.75
7	3	C	N	1.64	Q	32.20	564	3,800	942	3.53	.51
8	3	C	1/2	1.64	182	24.00	573	2,890	951	4.09	.62
9	1	C	N	1.30	129	33.30	546	2,770	988	3.47	.48
10	1	C	B	1.30	213	18.10	554	1,520	993	4.32	1.54
11	2	T	N	1.30	Q	42.00	549	3,490	990	3.48	.48
12	2	T	B	1.30	Q	40.40	560	3,430	1,003	2.43	.86
13	1	R	N	1.30	Q	39.40	565	3,370	1,005	3.19	.66
14	1	R	B	1.30	Q	38.60	560	3,270	1,003	2.57	.91
15	5	C	1/4	1.30	129	23.40	555	2,200	1,005	4.62	1.04
16	5	R	1/4	1.30	130	23.20	555	2,210	1,005	4.64	1.04
17	5	C	1/2	1.30	150	20.20	564	1,800	1,005	4.33	.60
18	8	C	B	1.64	256	19.60	549	2,263	928	3.38	1.26
19	7	C	N	1.64	Q	33.10	561	3,900	938	3.38	.40
20	6	C	N	2.00	250	22.55	579	3,488	881	4.05	.49
21	6	C	B	2.00	237	16.40	576	2,530	879	4.16	1.61

[a]Code used in table is defined as follows:

C model mount restrained
R model mount free to roll
T model mount free to translate
Q maximum dynamic pressure with no flutter
B wing without nacelles
N wing with normal nacelle configuration
1/4 outboard nacelle center of gravity at 0.25 chord
1/2 outboard nacelle center of gravity at 0.50 chord

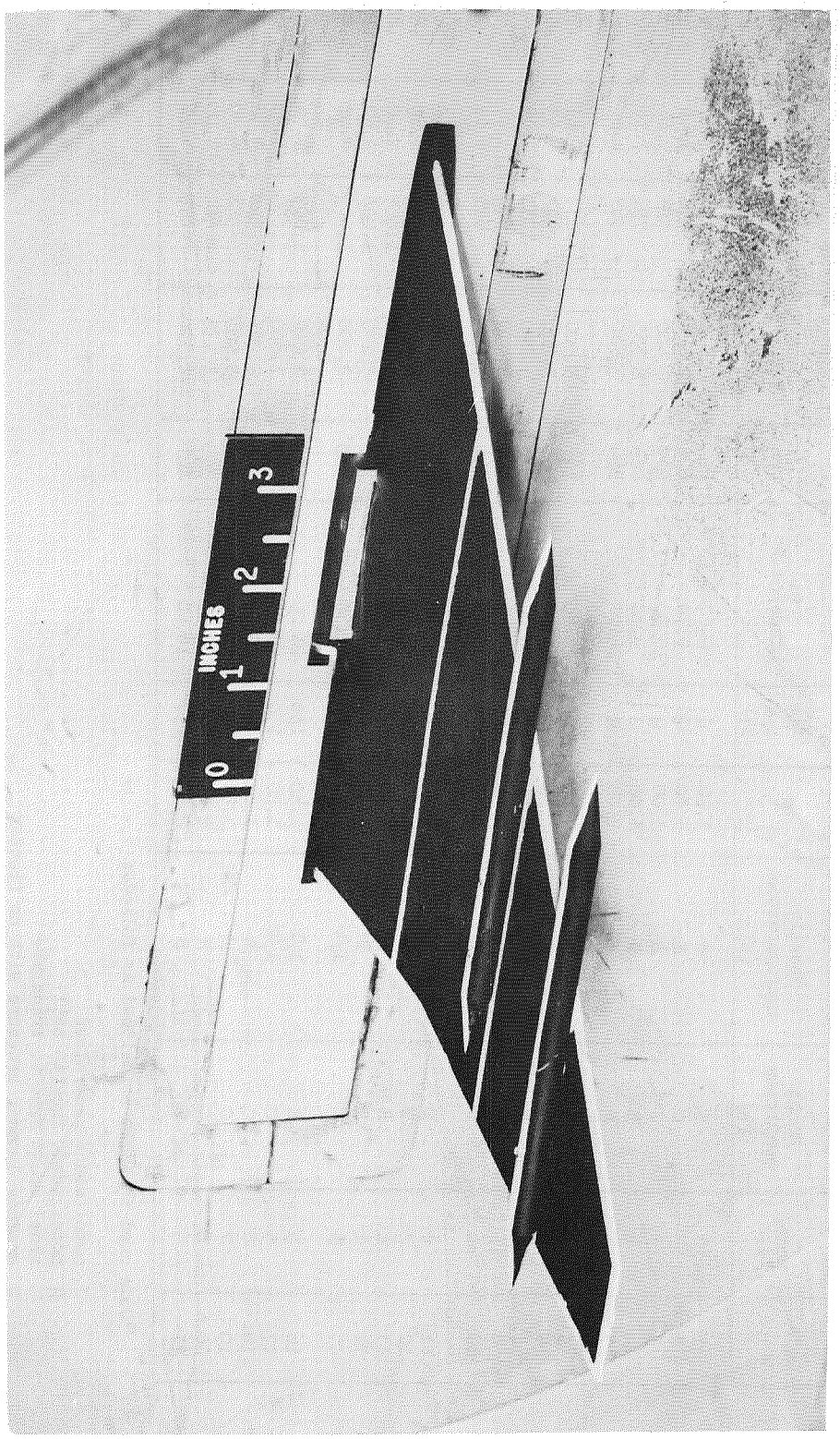

L-57-1104.1

Figure 1.- Photograph of model mounted in the Langley 9- by 18-inch supersonic flutter tunnel.

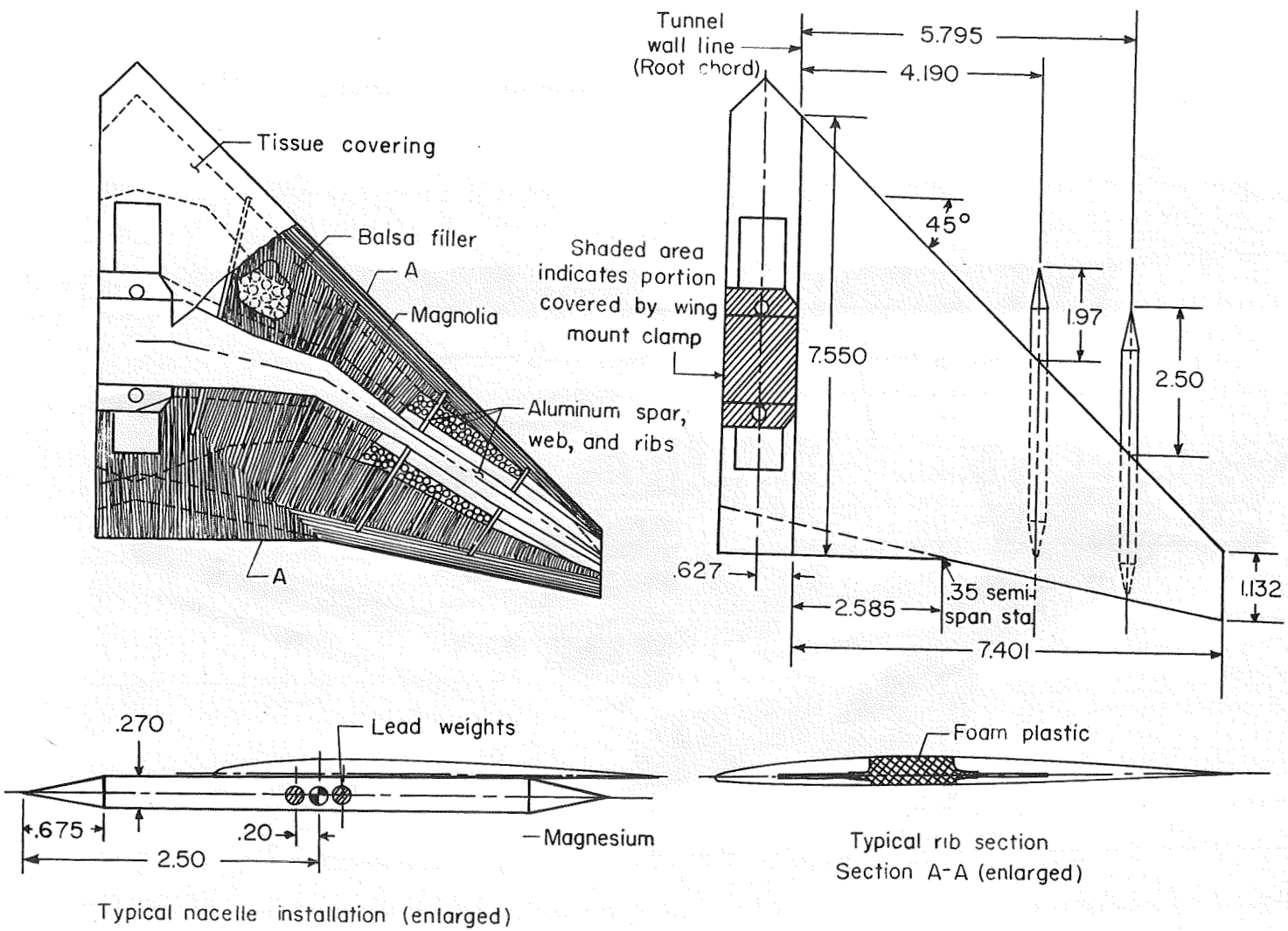

Figure 2.- Geometry and construction details of wing model and nacelles. Linear dimensions are in inches.

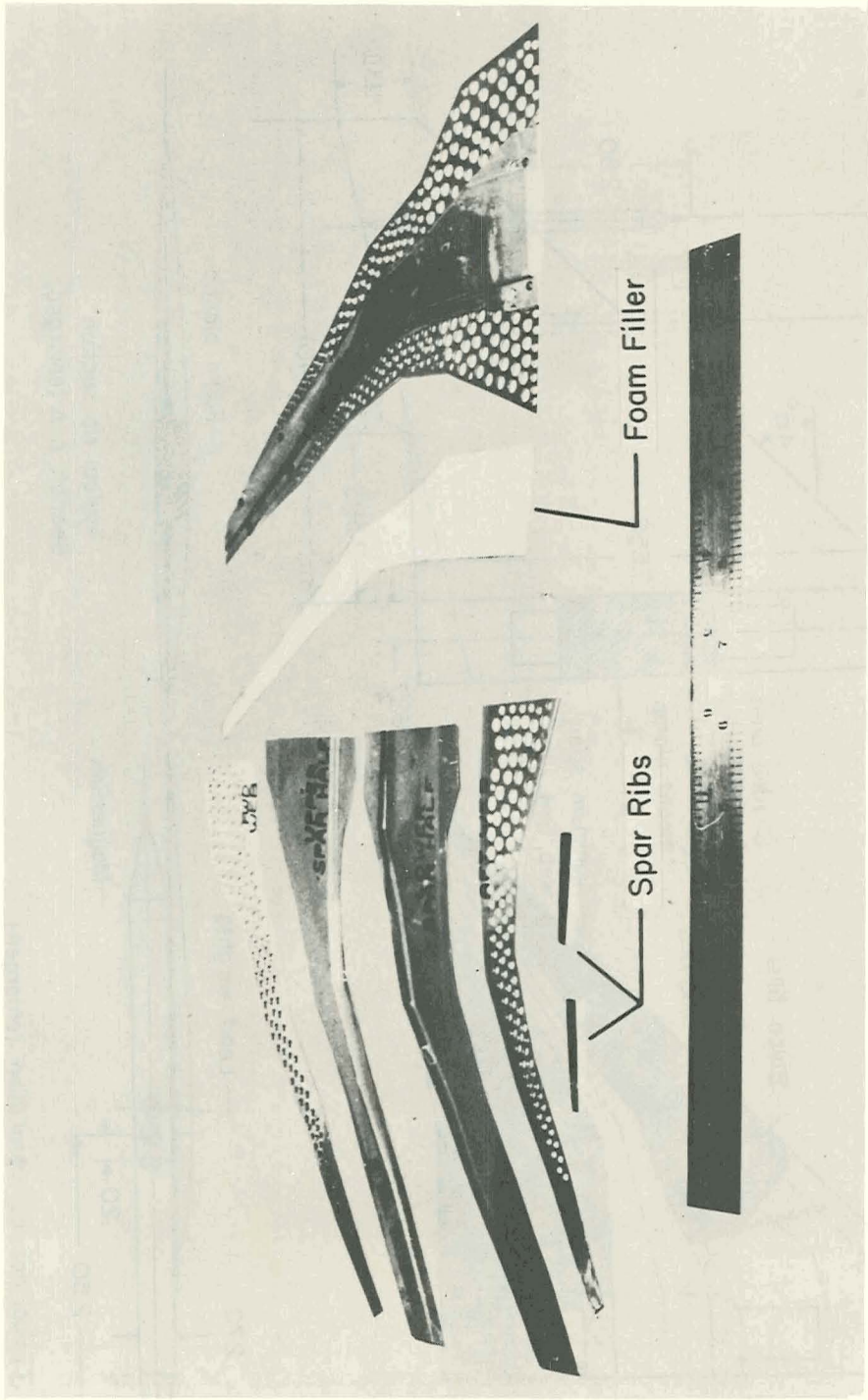

Figure 3.- Photograph of spar-web assembly. L-95187

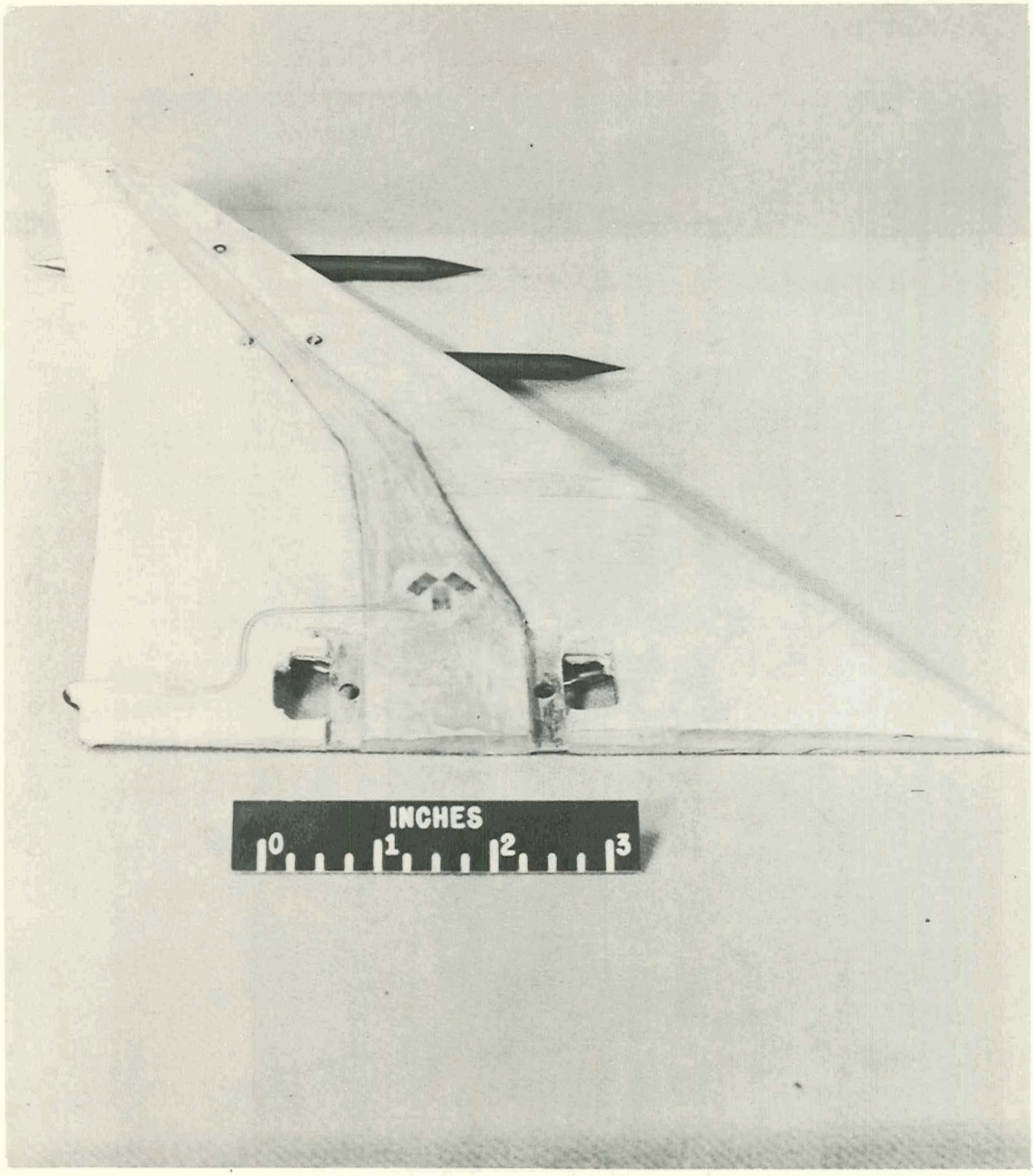

L-57-1107

Figure 4.- Photograph of model representative of models 6 to 9.

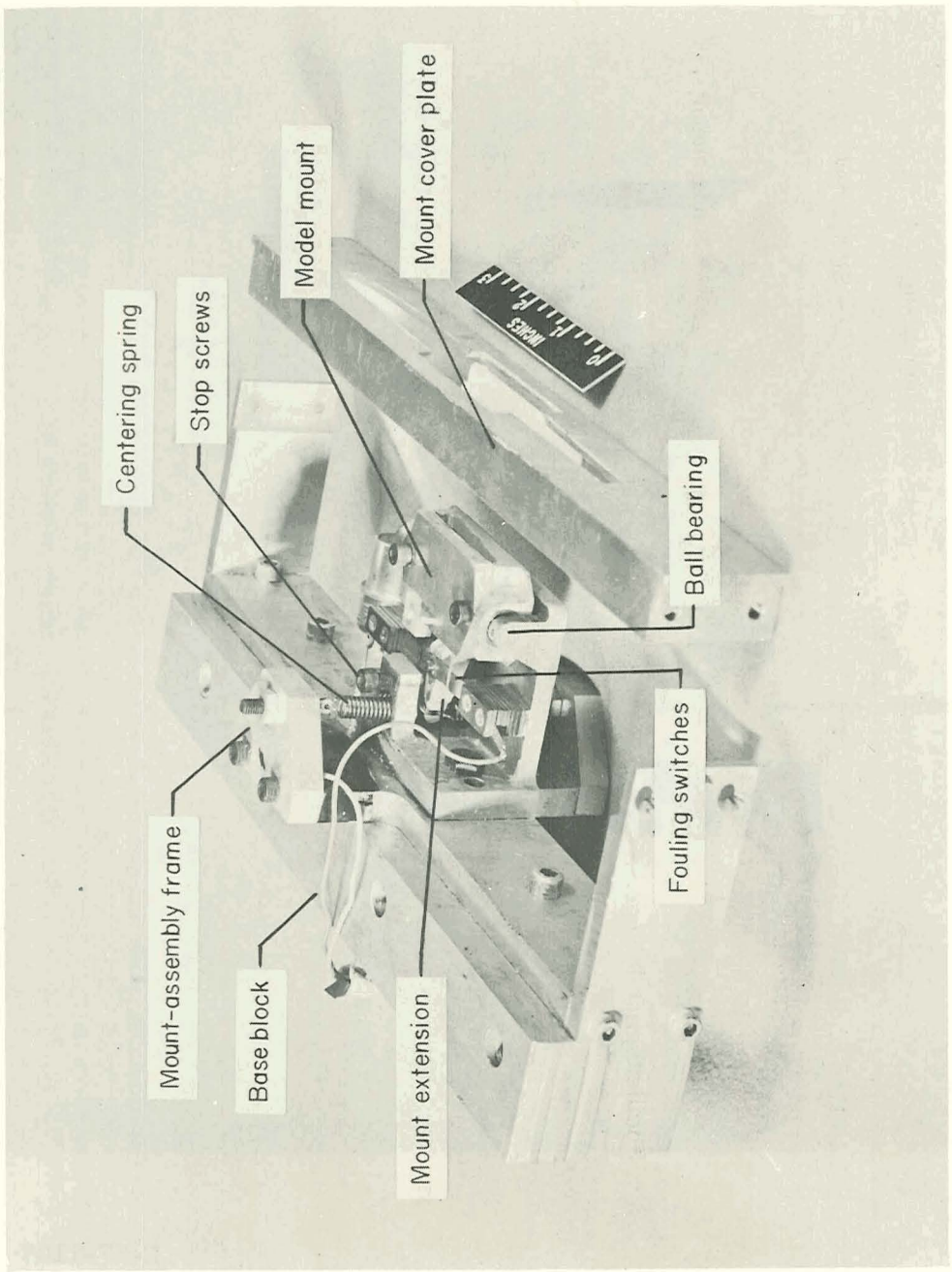

(a) Roll mount assembly. L-57-1106.1

Figure 5.- Photograph of model mount assemblies.

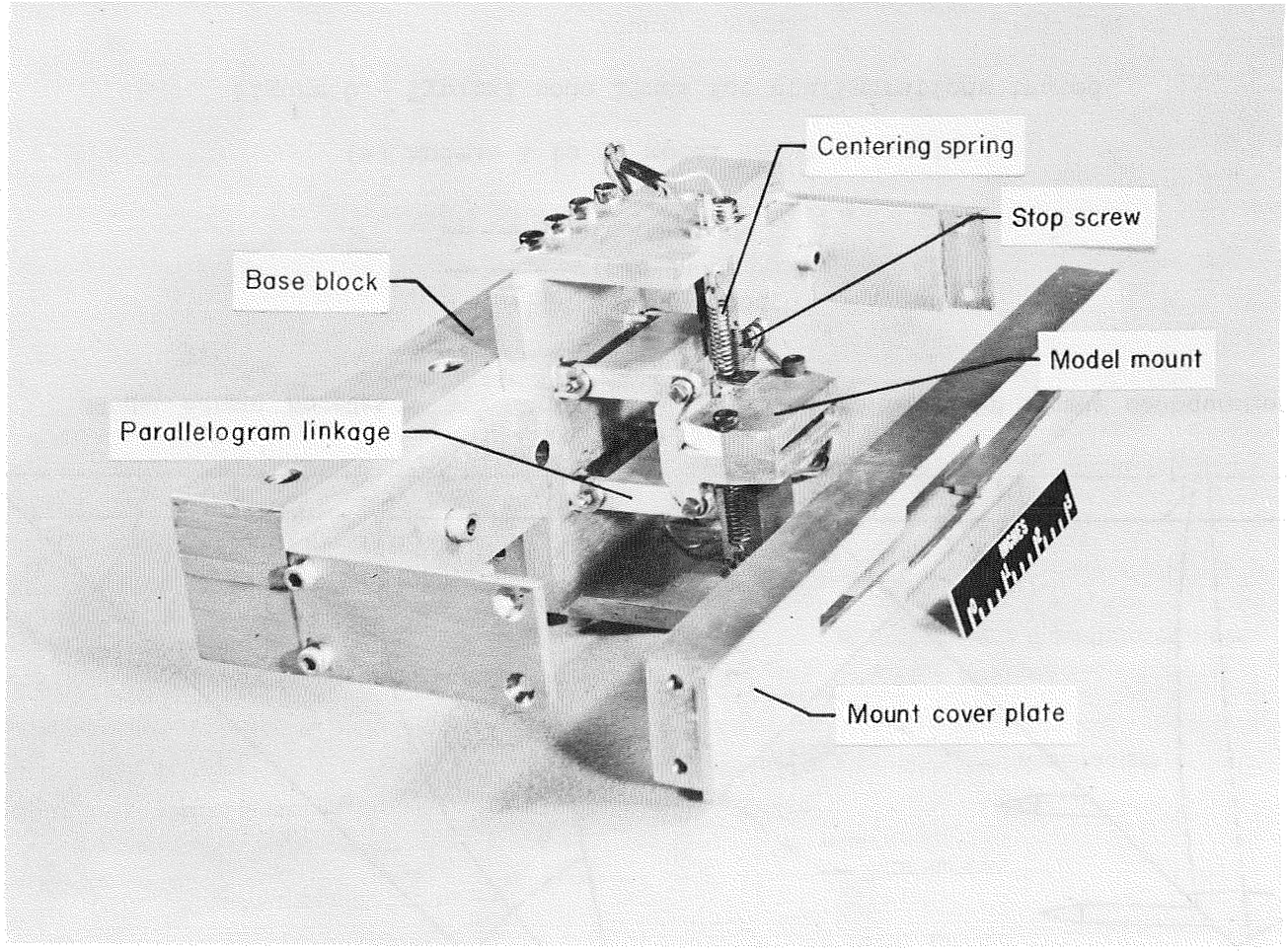

(b) Translation mount assembly. L-57-1105.1

Figure 5.- Concluded.

CONFIDENTIAL

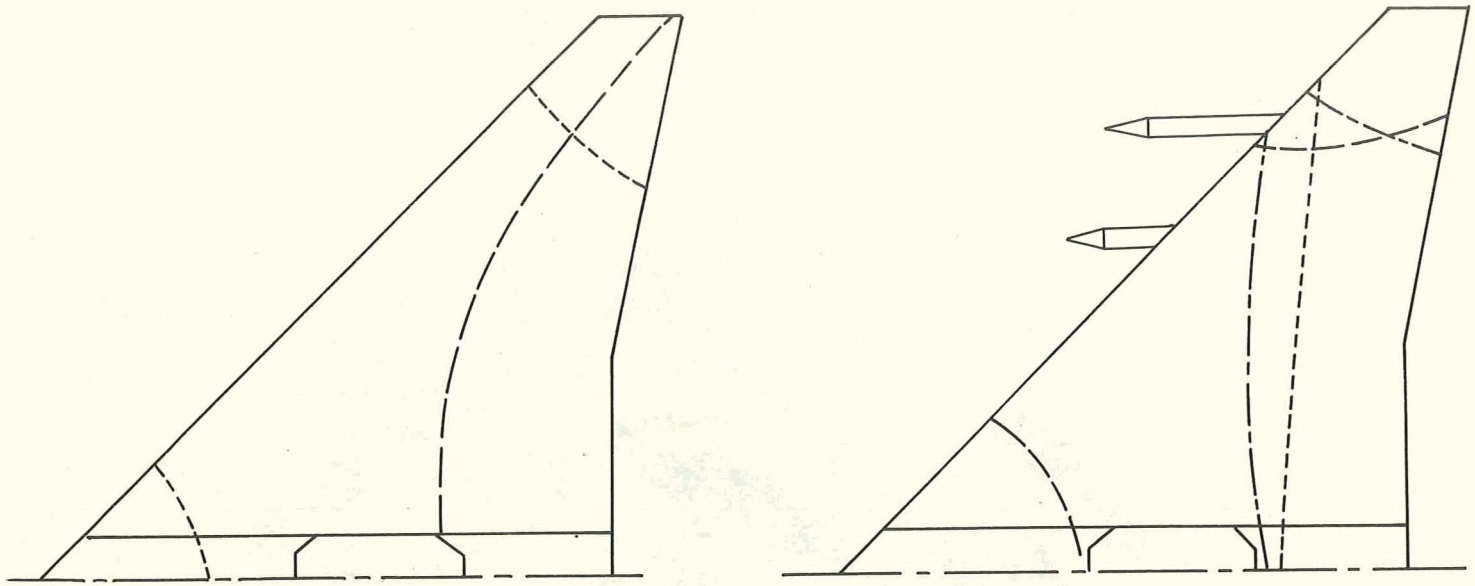

(a) Models 1 to 5; model mount restrained.

Figure 6.- Typical node lines for configurations tested.

CONFIDENTIAL

CONFIDENTIAL

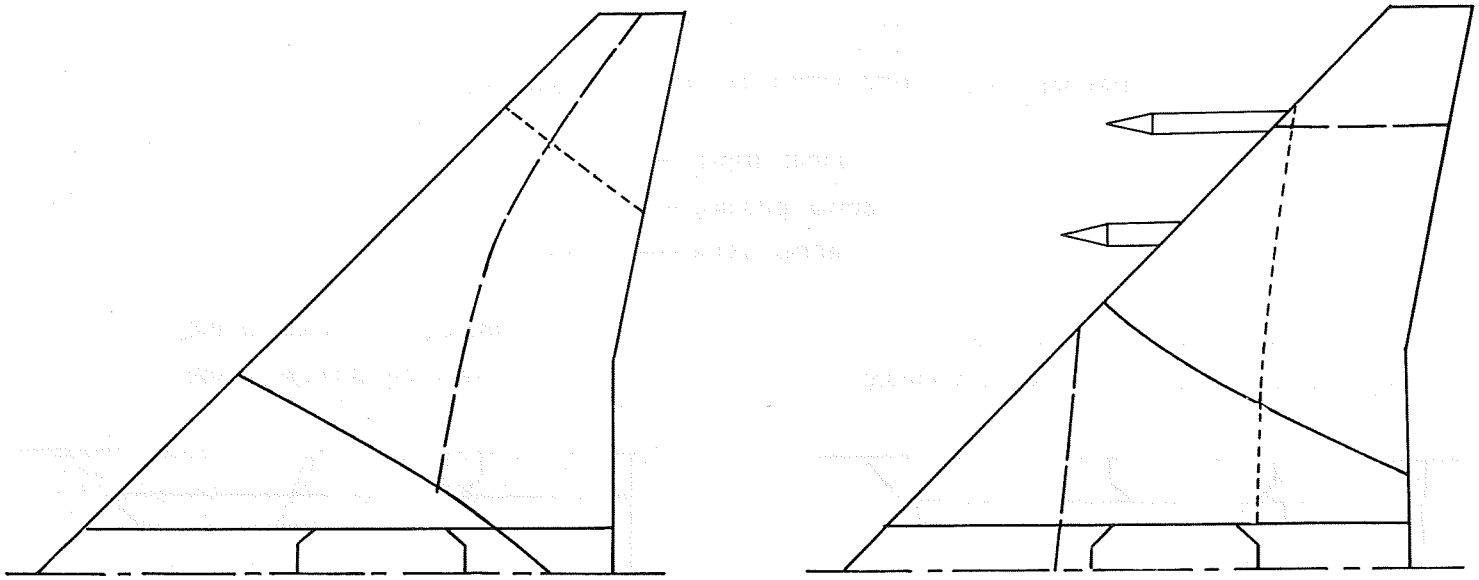

(b) Models 1 to 5; model mount free to translate.

Figure 6.- Continued.

CONFIDENTIAL

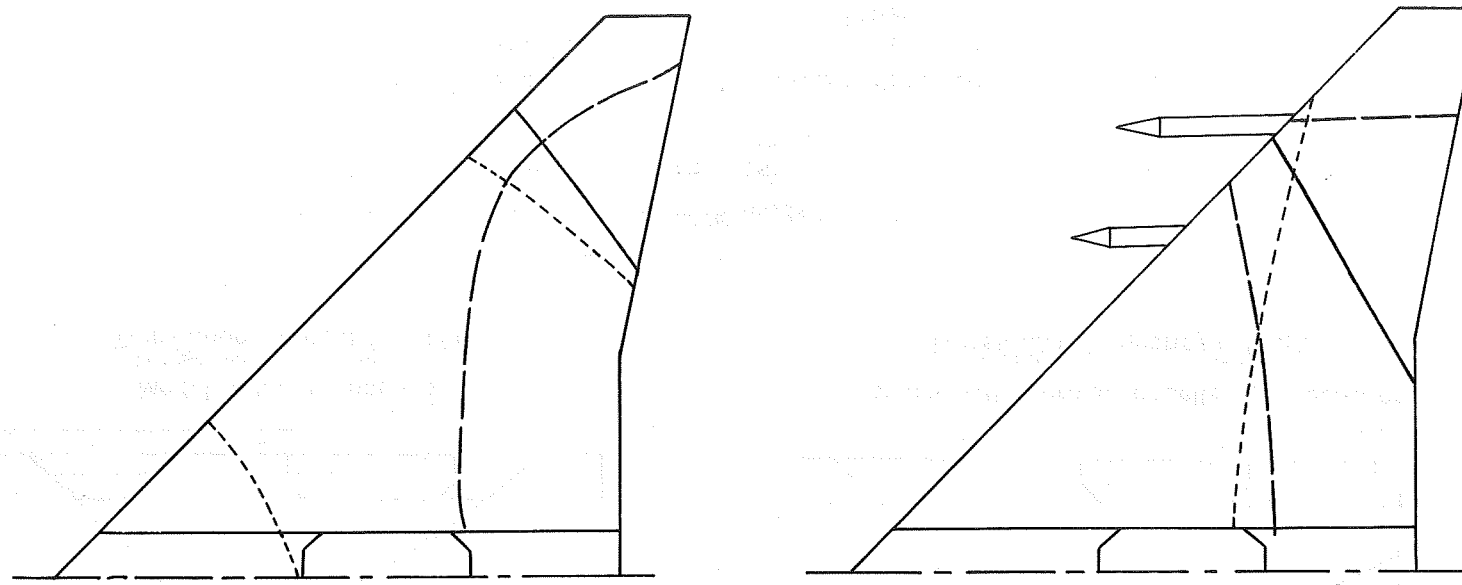

Model without nacelles
Roll frequency = 25 cps

Model with normal nacelle configuration
Roll frequency = 10 cps

——— First mode
------- Second mode
—— —— Third mode

(c) Models 1 to 5; model mount free to roll.

Figure 6.- Continued.

CONFIDENTIAL

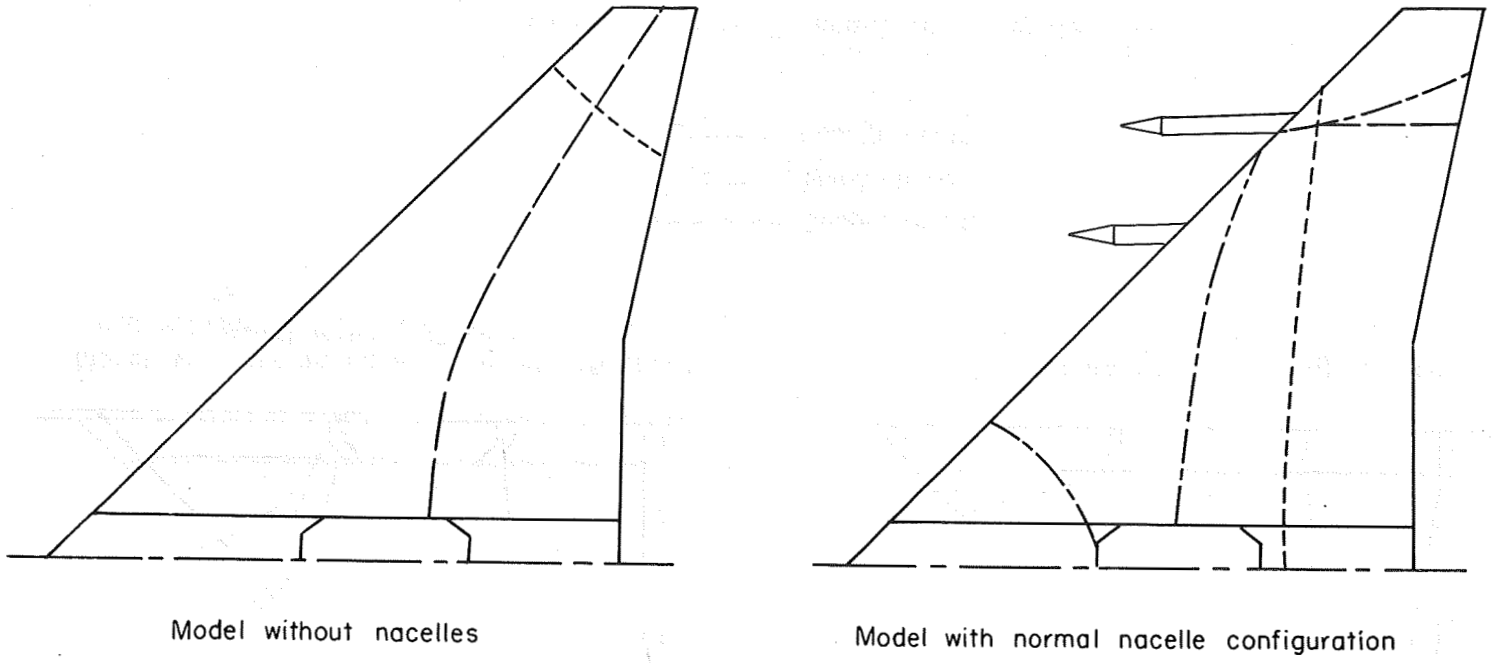

(d) Models 6 to 8; model mount restrained.

Figure 6.- Continued.

CONFIDENTIAL

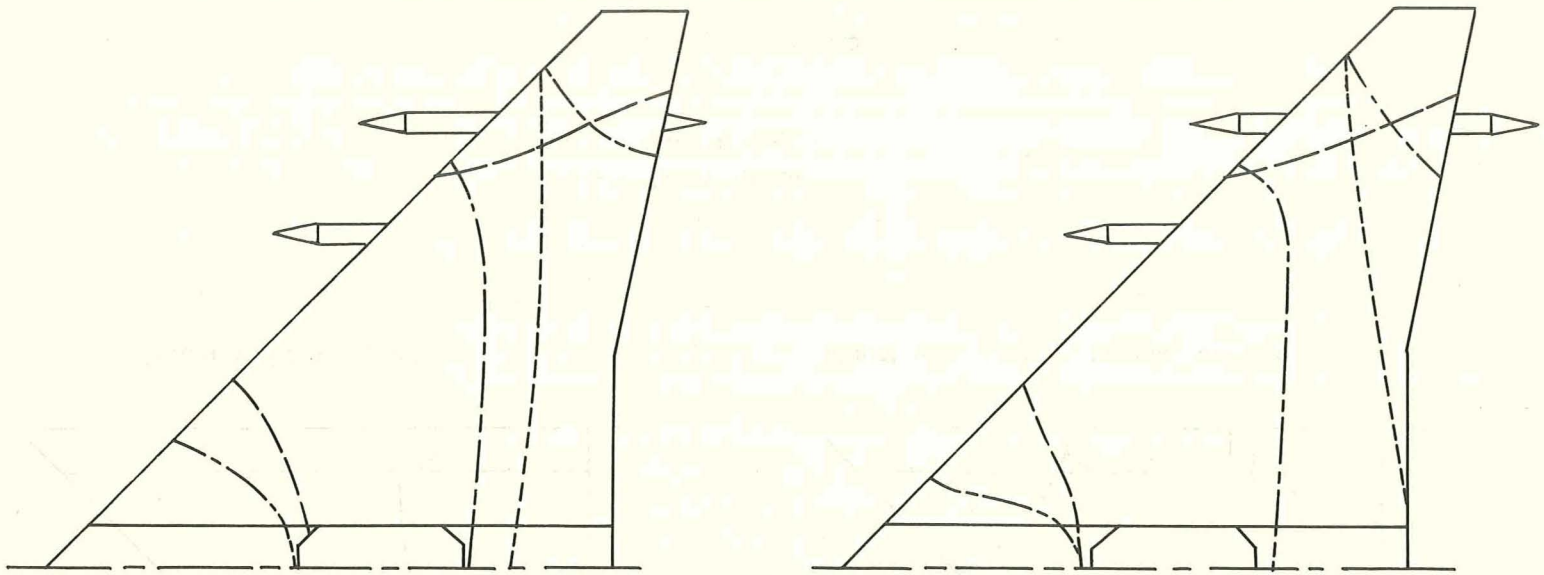

Model with inboard nacelle c.g. at .25 chord and outboard nacelle c.g. at .25 chord

Model with inboard nacelle c.g. at .25 chord and outboard nacelle c.g. at .50 chord

------- Second mode
— — — Third mode
—·—·— Fourth mode

(e) Models 6 to 8; model mount restrained.

Figure 6.- Concluded.

CONFIDENTIAL

CONFIDENTIAL

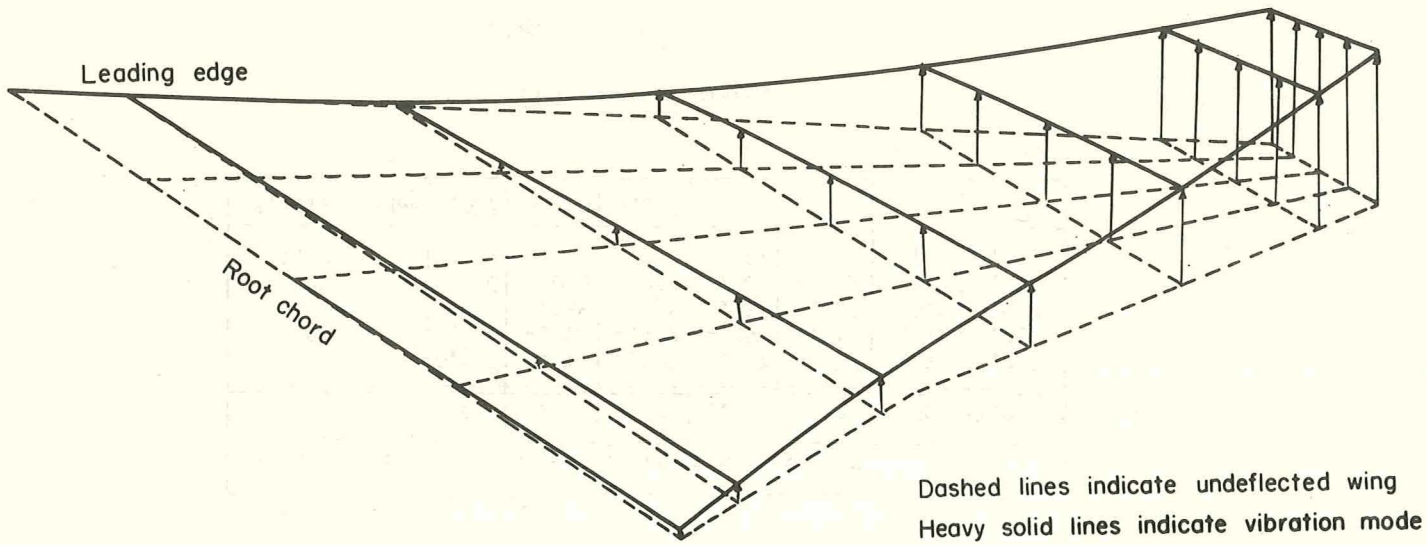

Fraction of chord	Normalized deflection at y/l =						
	0	0.10	0.30	0.50	0.70	0.90	1.00
0.00	0	.002	.037	.170	.420	.718	.868
.25	0	.008	.067	.230	.472	.754	.900
.50	0	.020	.109	.290	.523	.794	.933
.75	.005	.035	.159	.348	.575	.835	.968
1.00				.400	.623	.872	1.000
Trailing edge	.035	.075	.212				

(a) First mode.

Figure 7.- Representative mode shapes of wings 1 to 5 without nacelles with model mount restrained.

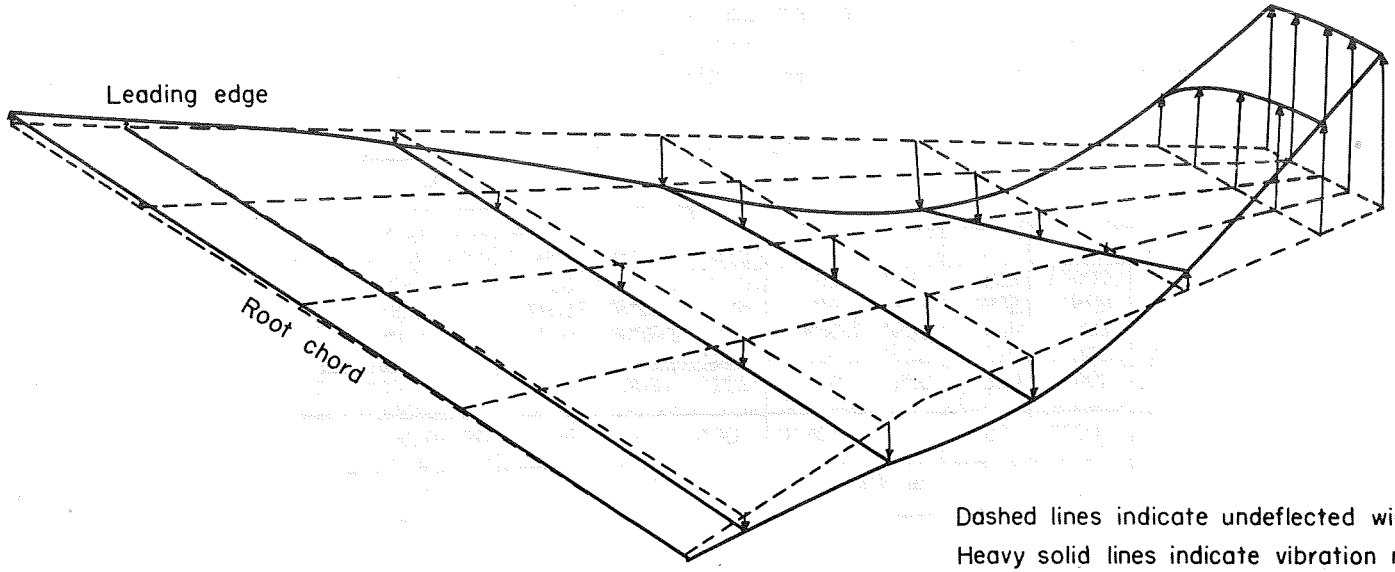

Fraction of chord	Normalized deflection at y/ℓ =						
	0	0.10	0.30	0.50	0.70	0.90	1.00
0.00	0.055	.016	-.095	-.327	-.445	.315	.926
.25	.012	-.024	-.122	-.291	-.315	.512	.960
.50	0	-.035	-.158	-.276	-.189	.614	.978
.75	-.008	-.050	-.209	-.284	-.039	.677	.992
1.00				-.307	+.118	.709	1.000
Trailing edge	-.047	-.110	-.276				

(b) Second mode.

Figure 7.- Continued.

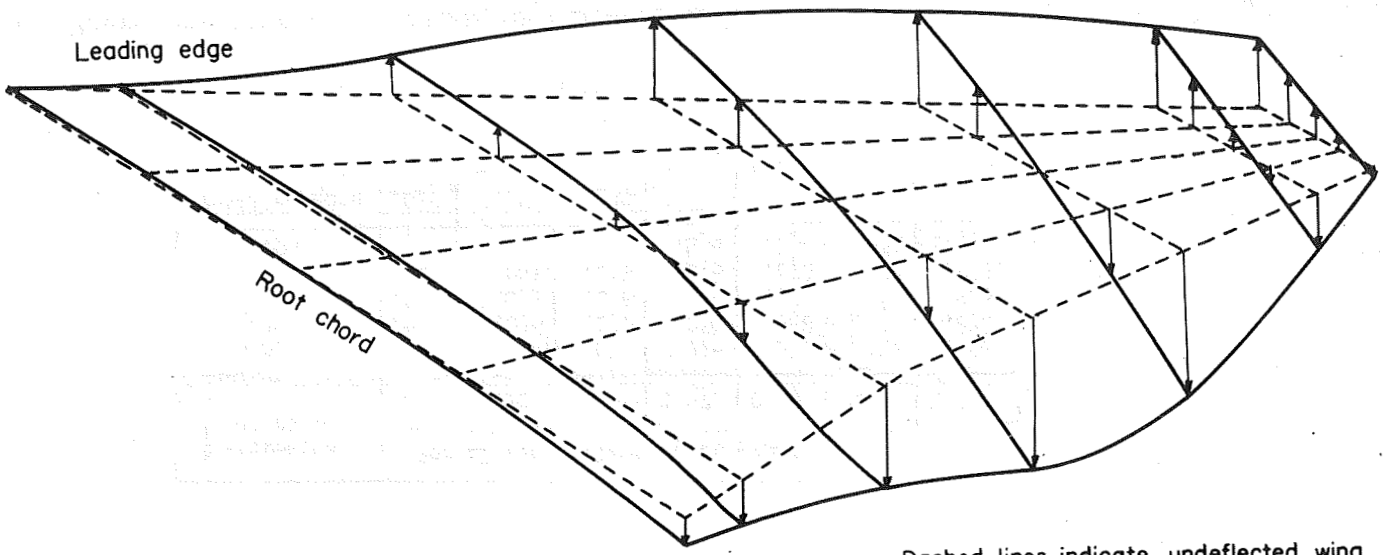

Fraction of chord	Normalized deflection at y/ℓ =						
	0	0.10	0.30	0.50	0.70	0.90	1.00
0.00	+.009	+.032	+.248	+.532	+.586	+.541	+.451
.25	+.014	+.050	+.203	+.338	+.338	+.334	+.325
.50	+.009	+.036	+.077	0	-.045	+.108	+.198
.75	-.018	-.041	-.279	-.442	-.406	-.117	+.063
1.00				-1.000	-.955	-.347	-.072
Trailing edge	-.176	-.298	-.694				

(c) Third mode.

Figure 7.- Concluded.

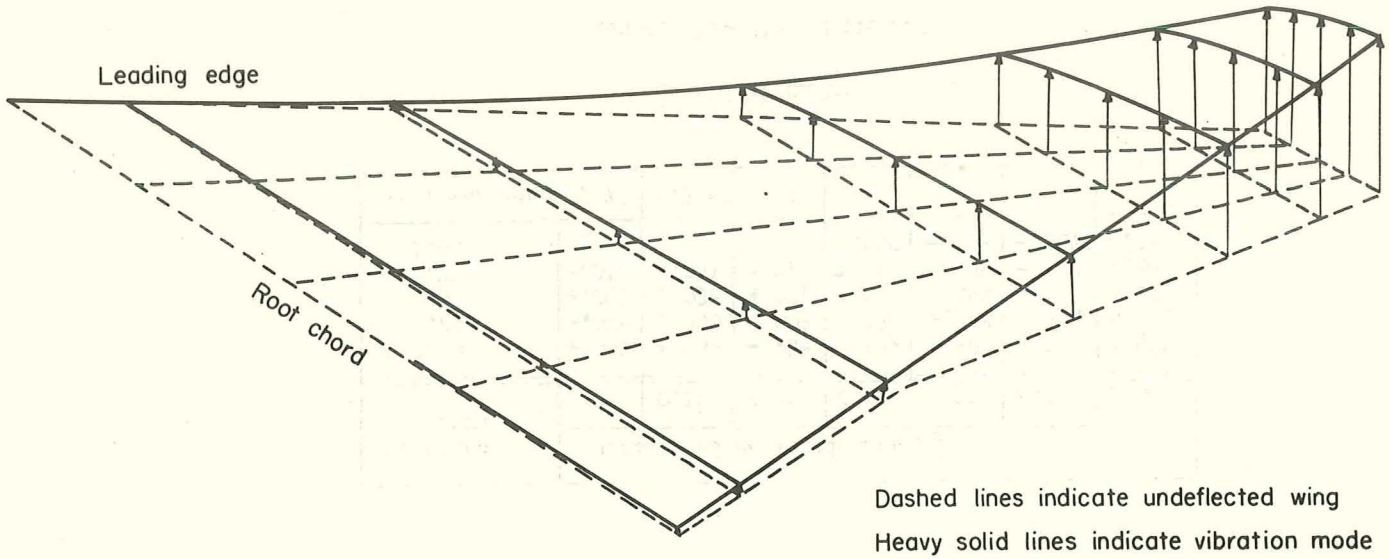

Fraction of chord	Normalized deflection at $y/\ell =$						
	0	0.10	0.30	0.57	0.78	0.90	1.00
0.00	0	.010	.057	.226	.471	.643	.796
.25	.006	.026	.070	.280	.548	.726	.878
.50	.013	.035	.096	.338	.624	.783	.923
.75	.019	.041	.115	.376	.672	.827	.962
1.00				.408	.704	.860	1.000
Trailing edge	.029	.057	.137				

(a) First mode.

Figure 8.- Representative mode shapes of wings 1 to 5 with nacelles in the normal configuration with model mount restrained.

CONFIDENTIAL

CONFIDENTIAL

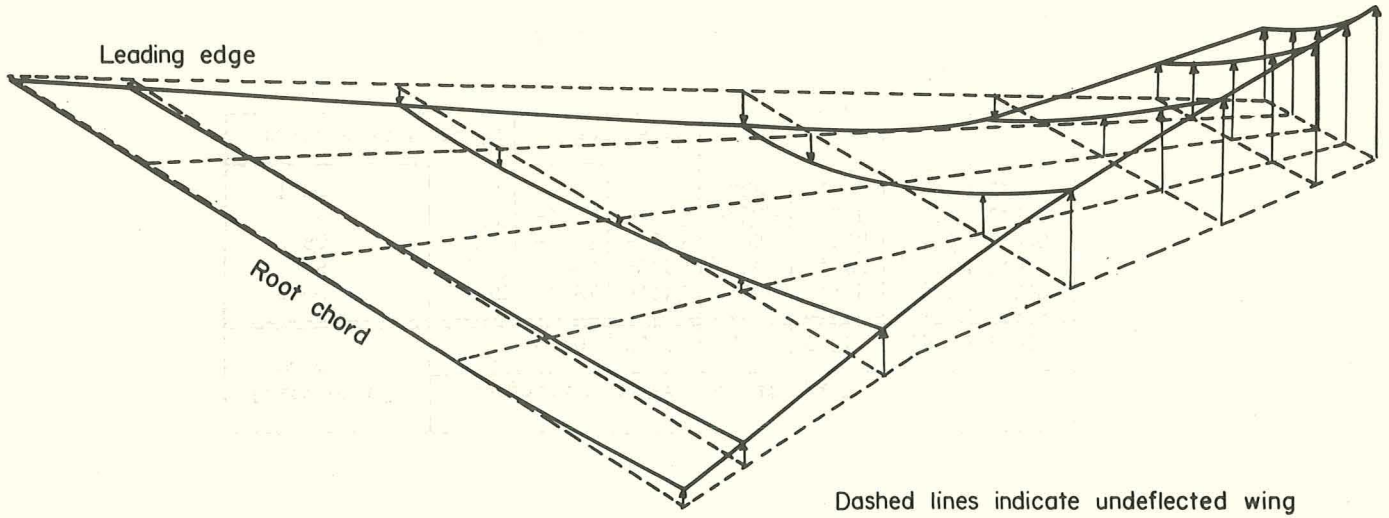

Fraction of chord	Normalized deflection at y/ℓ =						
	0	0.10	0.30	0.57	0.78	0.90	1.00
0.00	0.010	.028	.130	.240	.150	-.240	-.490
.25	.010	.026	.115	.170	-.040	-.370	-.560
.50	.010	.020	.070	0	-.255	-.520	-.660
.75	-.010	-.025	-.070	-.240	-.530	-.700	-.780
1.00				-.640	-.830	-.900	-1.000
Trailing edge	-.110	-.160	-.300				

(b) Second mode.

Figure 8.- Continued.

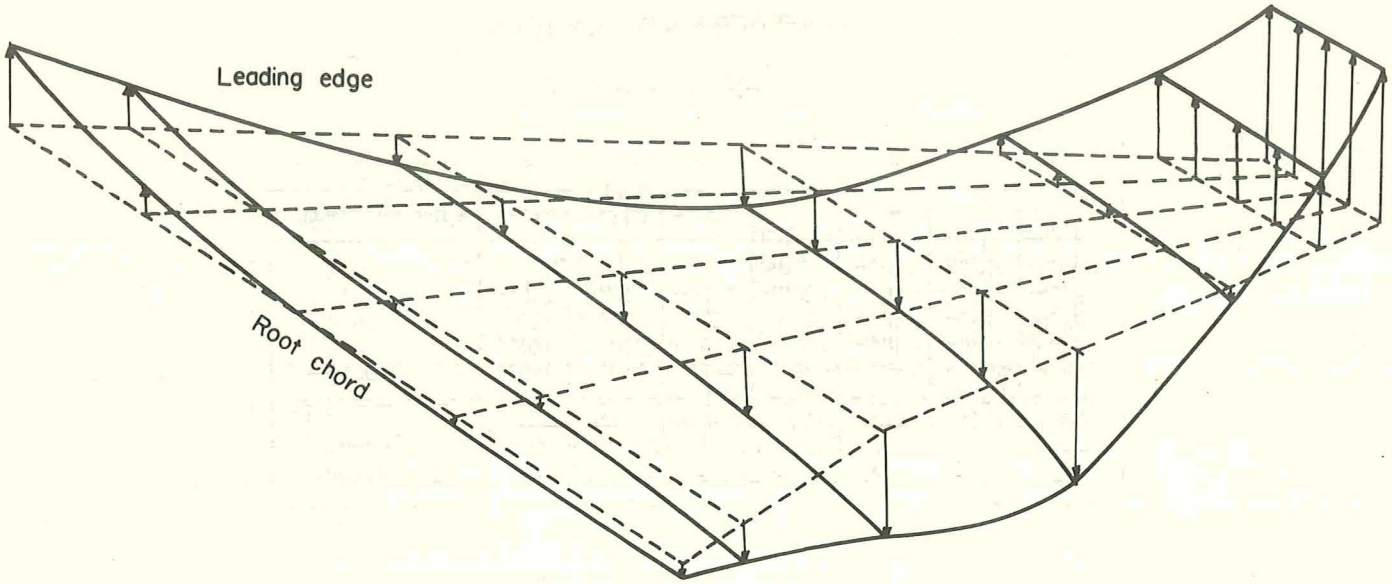

Dashed lines indicate undeflected wing
Heavy solid lines indicate vibration mode

Fraction of chord	Normalized deflection at y/ℓ =						
	0	0.10	0.30	0.57	0.78	0.90	1.00
0.00	0.532	.291	-.184	-.404	.129	.565	1.000
.25	.178	.048	-.226	-.404	.123	.548	1.000
.50	0	-.065	-.313	-.445	.084	.526	1.000
.75	-.048	-.129	-.436	-.549	.016	.500	1.000
1.00				-.887	-.097	.477	1.000
Trailing edge	-.097	-.258	-.694				

(c) Third mode.

Figure 8.- Continued.

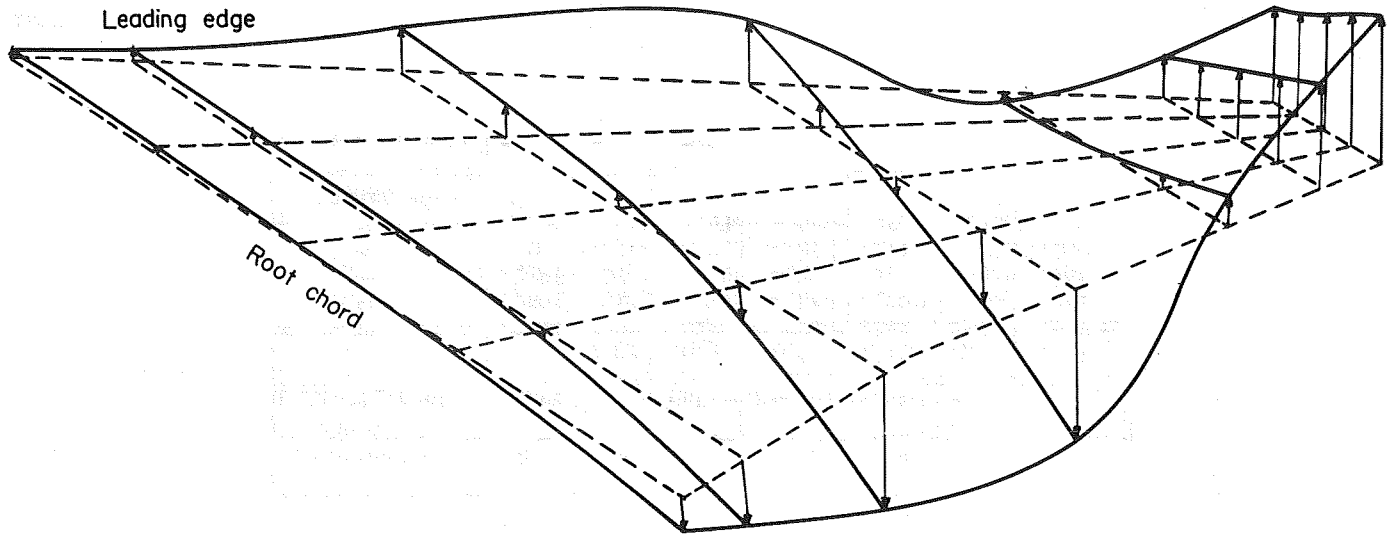

Dashed lines indicate undeflected wing
Heavy solid lines indicate vibration mode

Fraction of chord	Normalized deflection at y/ℓ =						
	0	0.10	0.30	0.57	0.78	0.90	1.00
0.00	0.052	.083	.277	.415	-.062	.283	.631
.25	.022	.077	.215	.194	-.043	.383	.692
.50	.015	.046	.077	-.154	0	.462	.769
.75	-.025	-.068	-.246	-.538	.077	.569	.861
1.00				-1.000	.200	.661	.954
Trailing edge	-.200	-.415	-.923				

(d) Fourth mode.

Figure 8.- Concluded.

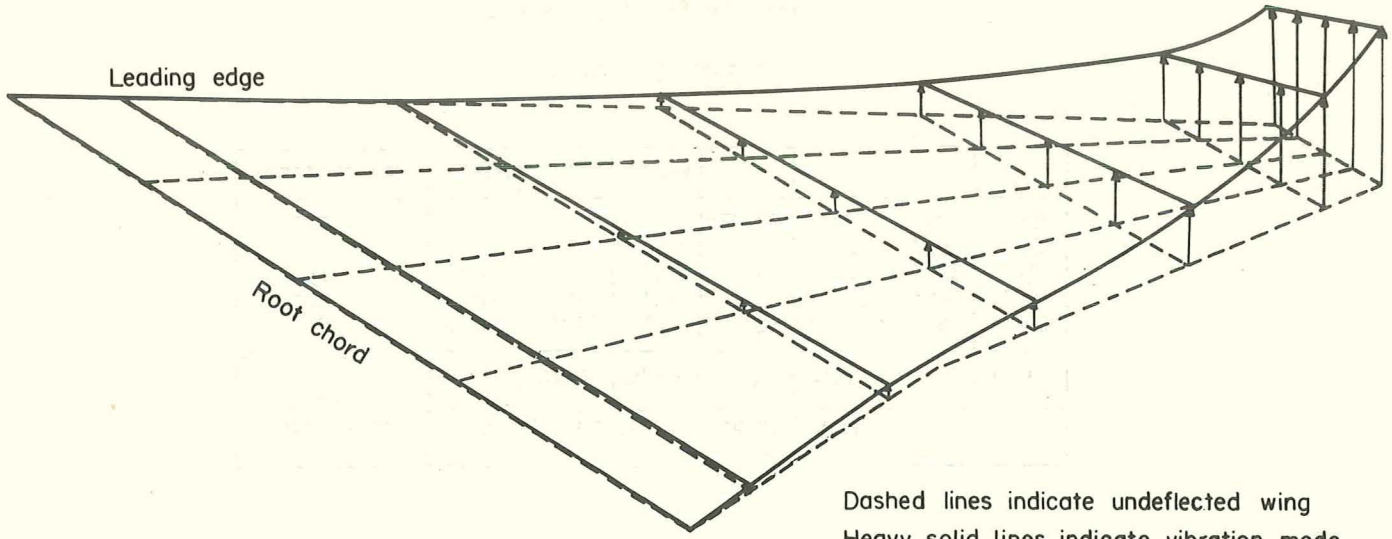

Fraction of chord	Normalized deflection at y/ℓ =						
	0	0.10	0.30	0.50	0.70	0.90	1.00
0.00	0.002	.003	.023	.090	.215	.449	.767
.25	.004	.009	.038	.115	.241	.509	.818
.50	.006	.013	.054	.143	.276	.580	.881
.75	.009	.020	.071	.166	.310	.646	.946
1.00				.192	.357	.719	1.000
Trailing edge	.023	.038	.094				

(a) First mode.

Figure 9.- Representative mode shapes of wings 6 to 9 without nacelles with model mount restrained.

CONFIDENTIAL

CONFIDENTIAL

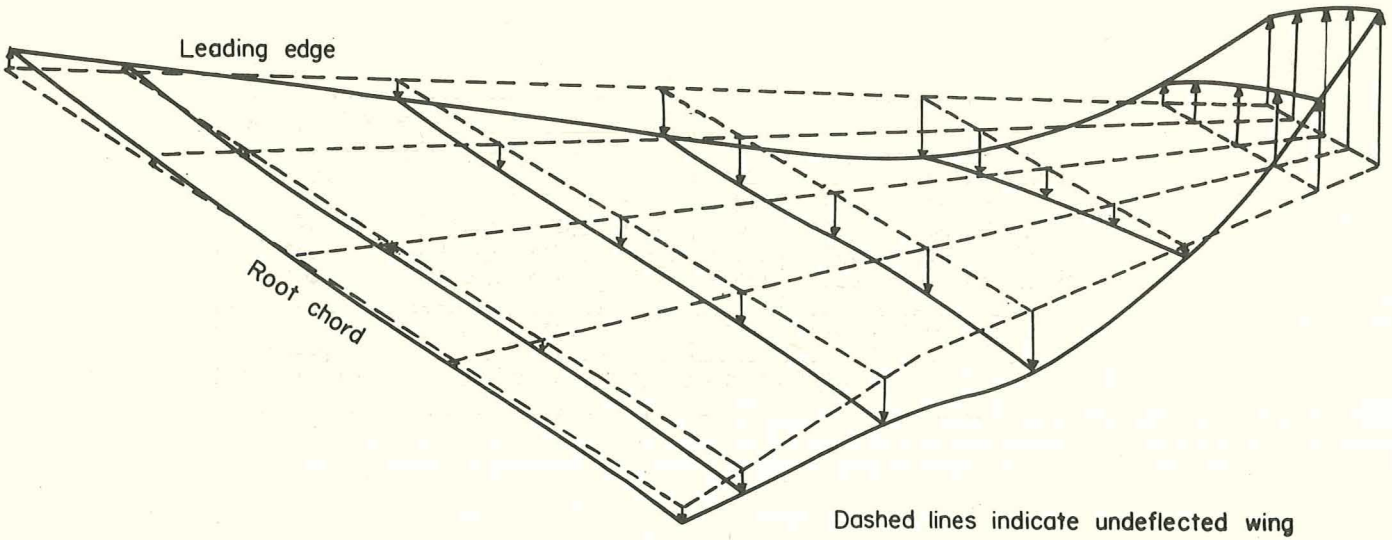

Fraction of chord	Normalized deflection at y/ℓ =						
	0	0.10	0.30	0.50	0.70	0.90	1.00
0.00	0.133	.044	-.133	-.304	-.400	.138	.571
.25	.051	-.036	-.187	-.320	-.291	.269	.700
.50	-.029	-.080	-.207	-.304	-.213	.382	.807
.75	-.049	-.104	-.233	-.304	-.129	.498	.929
1.00				-.398	-.069	.584	1.000
Trailing edge	-.100	-.176	-.324				

(b) Second mode.

Figure 9.- Continued.

CONFIDENTIAL

CONFIDENTIAL

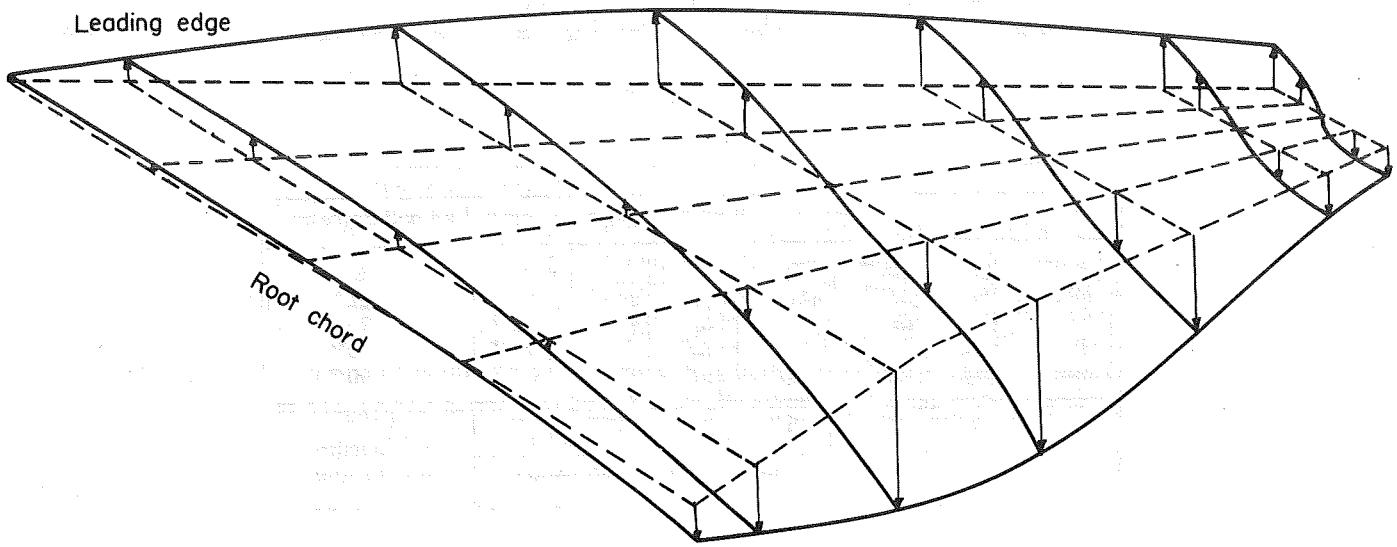

Dashed lines indicate undeflected wing
Heavy solid lines indicate vibration mode

Fraction of chord	Normalized deflections at y/ℓ =						
	0	0.10	0.30	0.50	0.70	0.90	1.00
0.00	+.040	+.145	+.352	+.471	+.456	+.346	+.291
.25	+.055	+.123	+.251	+.297	+.260	+.216	+.194
.50	+.022	+.099	+.062	-.077	-.150	-.100	-.080
.75	-.040	-.099	-.260	-.410	-.408	-.220	-.172
1.00				-1.000	-.670	-.282	-.176
Trailing edge	-.220	-.454	-.910				

(c) Third mode.

Figure 9.- Concluded.

CONFIDENTIAL

CONFIDENTIAL

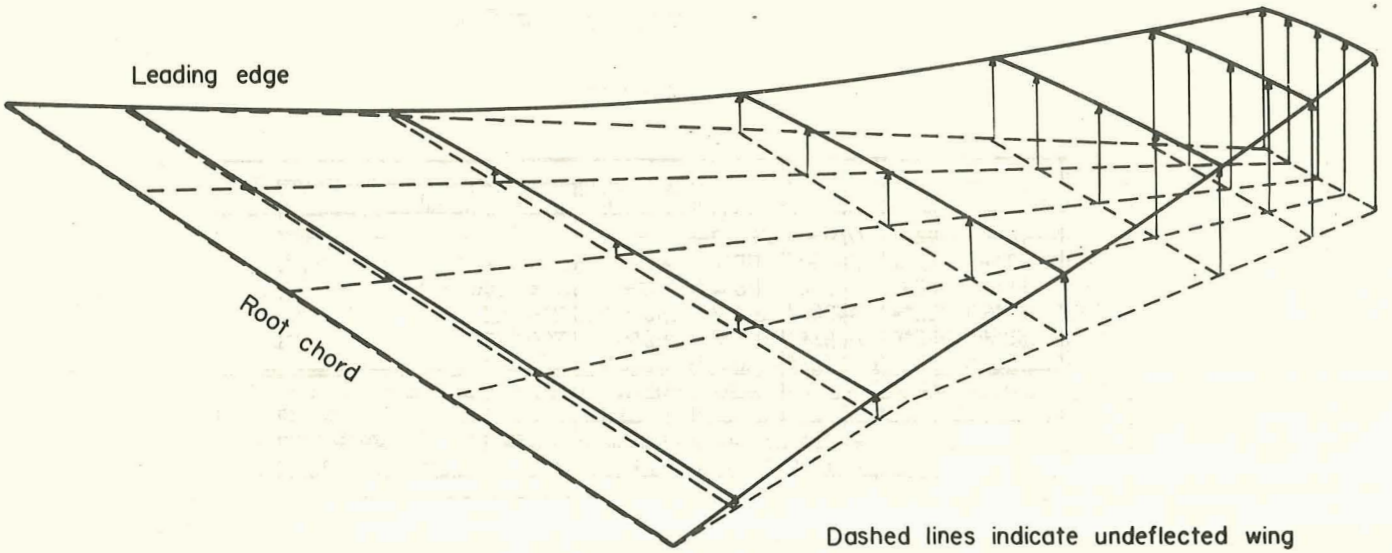

Fraction of chord	Normalized deflection at y/ℓ =						
	0	0.10	0.30	0.57	0.78	0.90	1.00
0.00	.003	.018	.057	.243	.553	.753	.908
.25	.002	.022	.075	.290	.594	.789	.938
.50	.001	.026	.093	.332	.637	.824	.965
.75	.001	.035	.119	.378	.667	.846	.982
1.00				.413	.695	.868	1.000
Trailing edge	.003	.053	.141				

(a) First mode.

Figure 10.- Representative mode shapes of wings 6 to 9 with nacelles in the normal configuration with model mount restrained.

CONFIDENTIAL

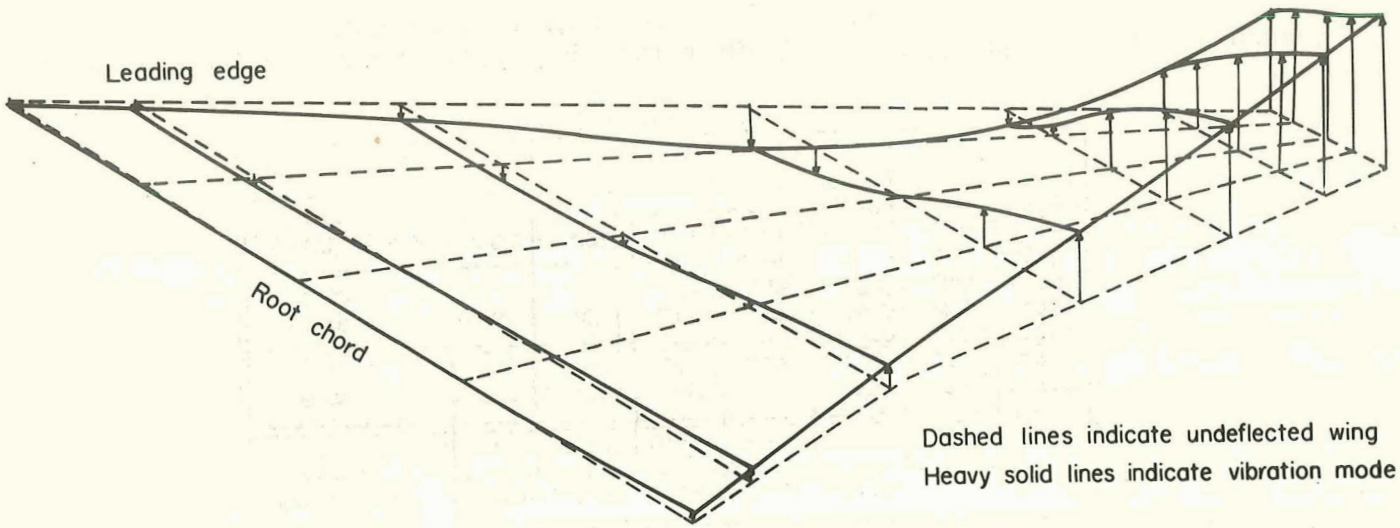

Fraction of chord	Normalized deflection at y/ℓ =						
	0	0.10	0.30	0.57	0.78	0.90	1.00
0.00	-.034	-.047	-.102	-.275	-.120	.238	.628
.25	-.034	-.047	-.095	-.175	.092	.452	.726
.50	-.014	-.029	-.082	.030	.375	.606	.809
.75	0	.007	.049	.257	.562	.735	.874
1.00				.455	.725	.881	1.000
Trailing edge	.048	.075	.149				

(b) Second mode.

Figure 10.- Continued.

CONFIDENTIAL

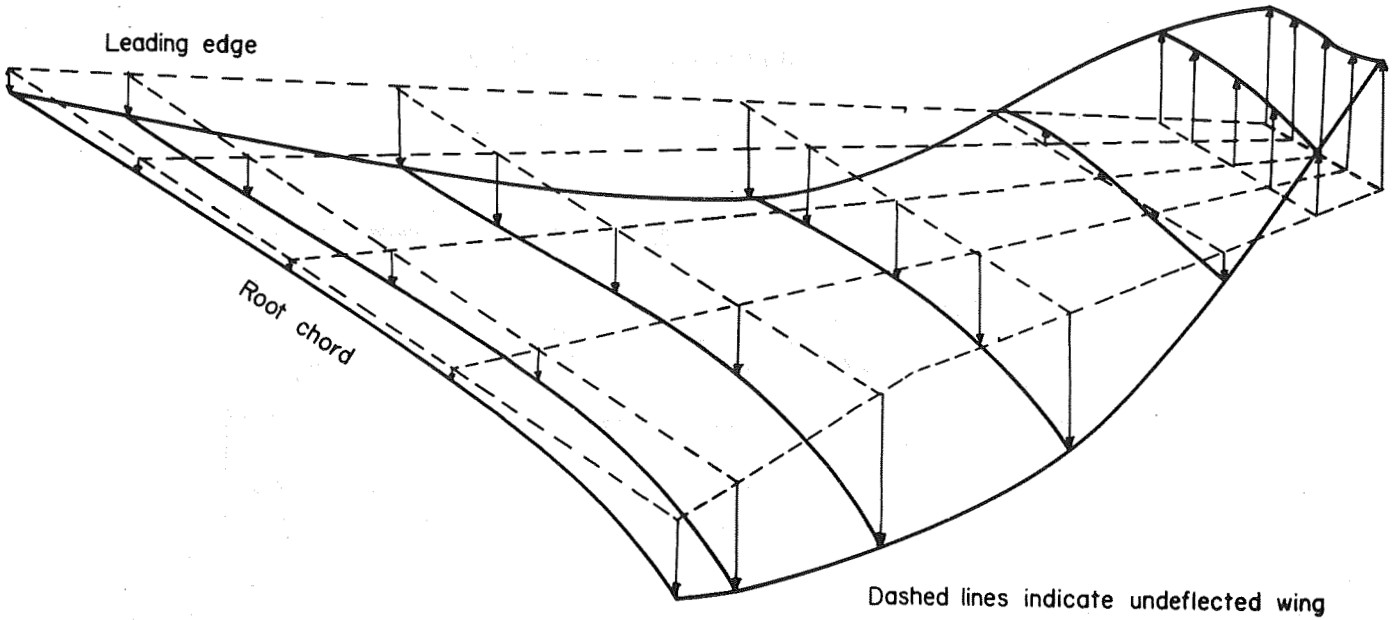

Fraction of chord	Normalized deflection at y/ℓ *						
	0	0.10	0.30	0.57	0.78	0.90	1.00
0.00	-.147	-.294	-.485	-.600	+.040	.603	.779
.25	-.132	-.274	-.468	-.525	+.090	.588	.779
.50	-.074	-.221	-.441	-.520	0	.571	.774
.75	-.088	-.221	-.482	-.610	-.120	.526	.756
1.00				-.920	-.240	.406	.756
Trailing edge	-.500	-.712	-1.000				

(c) Third mode.

Figure 10.- Continued.

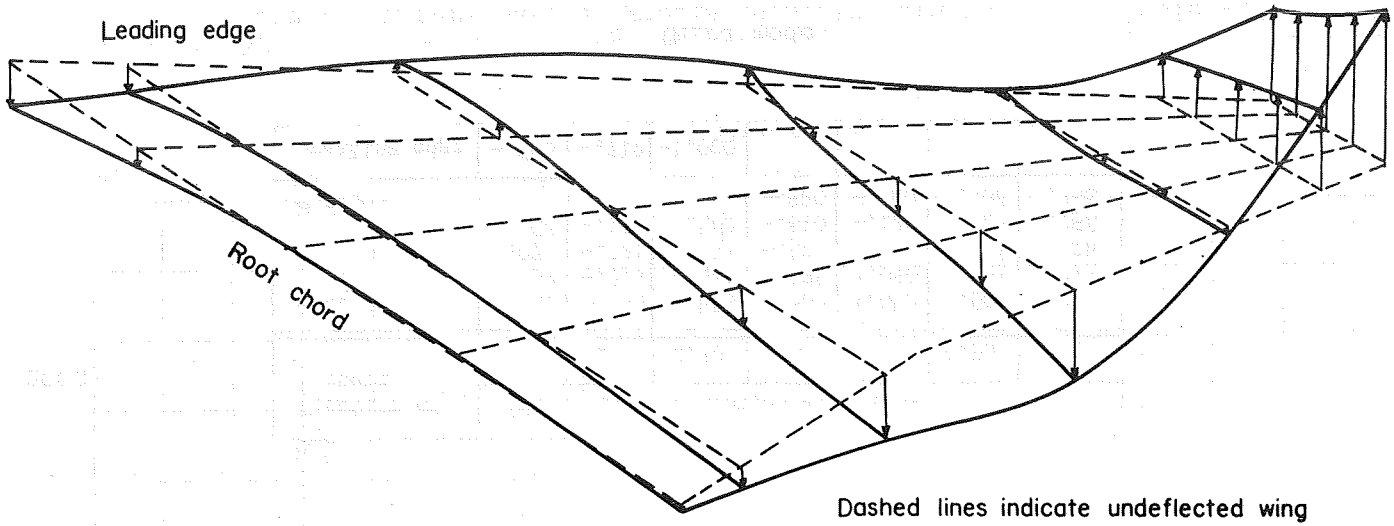

Fraction of chord	Normalized deflection at y/ℓ =						
	0	0.10	0.30	0.57	0.78	0.90	1.00
0.00	-.284	-.155	.091	.130	.060	.290	.615
.25	-.121	-.030	.081	-.100	-.045	.341	.673
.50	-.021	-.001	-.081	-.230	-.050	.394	.754
.75	-.014	-.053	-.239	-.375	-.055	.452	.861
1.00				-.590	-.060	.524	1.000
Trailing edge	-.050	-.146	-.443				

(d) Fourth mode.

Figure 10.- Concluded.

CONFIDENTIAL

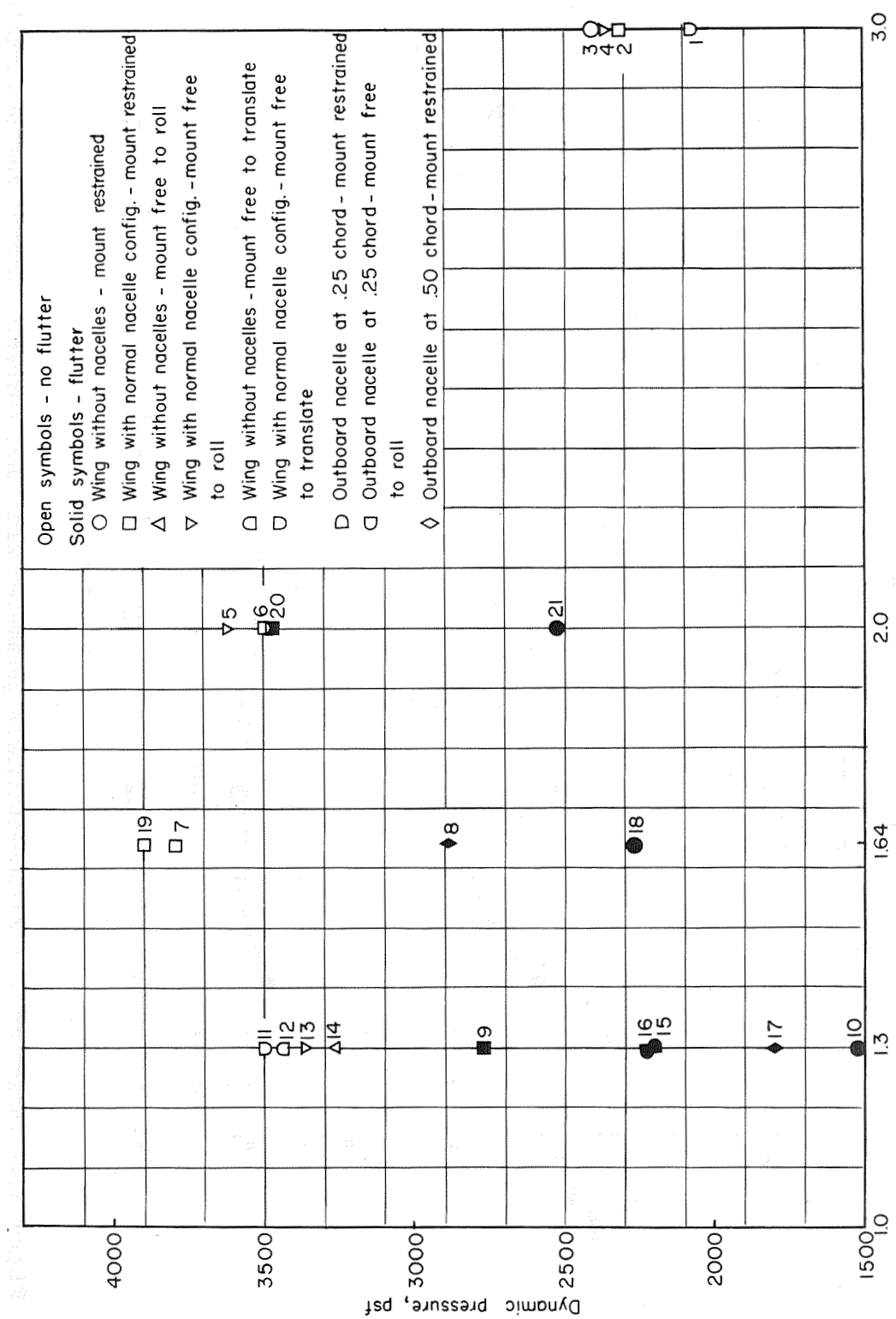

Figure 11.- Experimentally determined flutter characteristics of wings under all conditions tested. Numbers beside symbols identify data points in table VII.

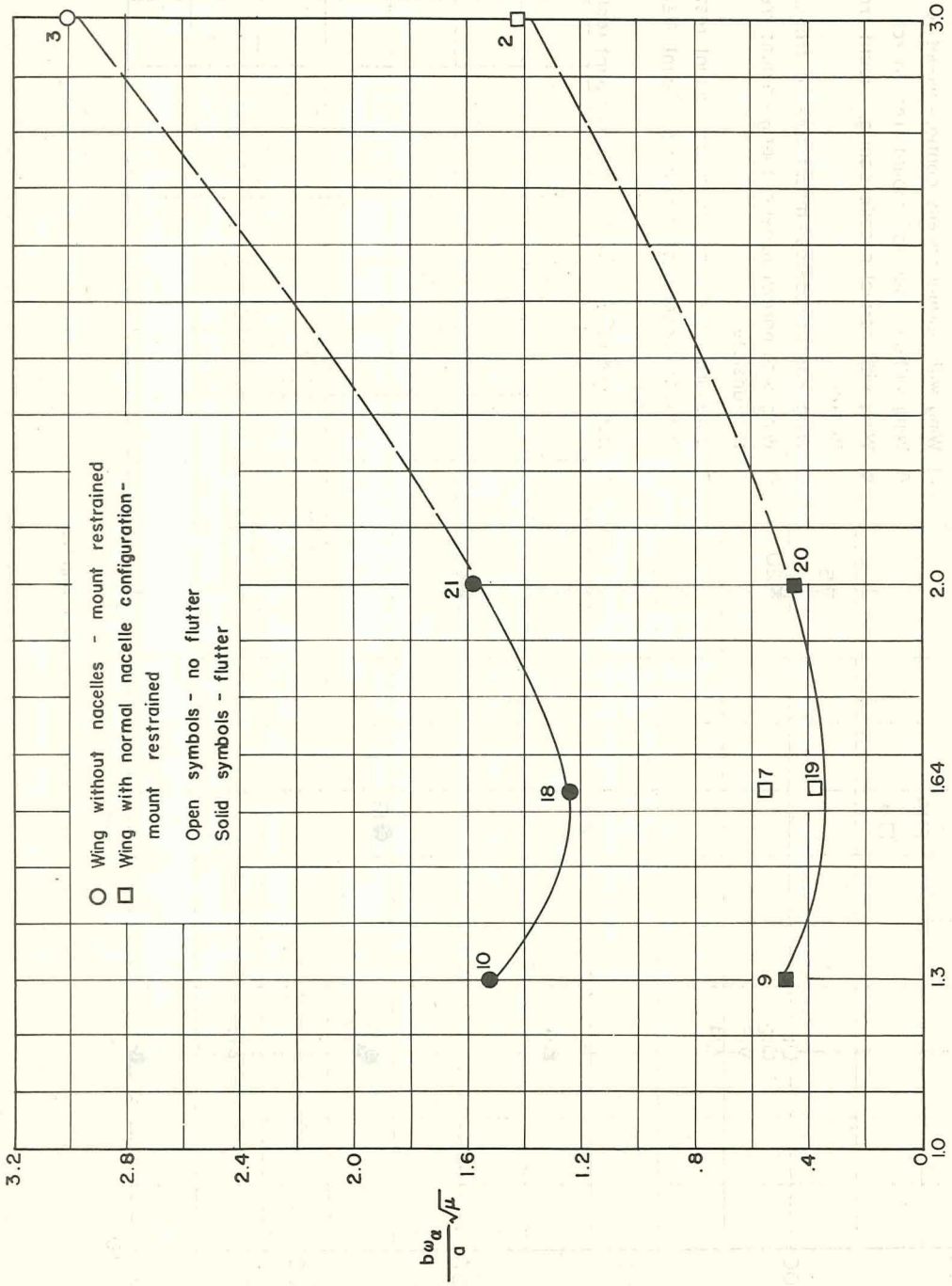

Figure 12.- Variation of altitude-stiffness parameter with Mach number. Numbers beside symbols identify data points in table VII.

NACA - Langley Field, Va.